POLITECNICO DI TORINO

Corso di Laurea in Ingegneria Aerospaziale

Tesi di Laurea Magistrale

Prognostic and Development of Methods for the Utilisation of Fibers as Advanced Sensors in Aeronautics

Relatori
Prof. Paolo Maggiore
Ing. Matteo Dalla Vedova

Candidato
Alice Sgroi

Marzo 2019

Ringraziamenti

I ringraziamenti più importanti li rivolgo alle persone che mi hanno accompagnato tutti i giorni nello svolgimento di questo lavoro di tesi. Primi fra tutti dunque il Prof.re Paolo Maggiore e l'Ing.Matteo D.L. Dalla Vedova, che mi hanno dato fiducia e permesso di prendere parte a questo importante progetto presso il *Laboratorio PhotoNext* del nostro *Politecnico di Torino*. Un ulteriore ringraziamento va al Dott. Piercarlo Berri, che è sempre stato disponibile a chiarimenti in ogni settore e a fornire ogni tipo di supporto necessario. Ringrazio anche il Dott. Matteo Facciano, dall'*Istituto Superiore Mario Boella*, per averci sempre fornito tutto il fabbisogno di fibre ottiche e incollaggi vari, oltre che un supporto su cui contare sempre. Un ringraziamento va anche al *Team Icarus* per la costante disponibilità a collaborazioni, in particolare nella persona di Michele Mabritto. Infine, ma non per questo meno importanti, non posso non ringraziare tutti i ragazzi con cui ogni giorno ci siamo trovati a lavorare, studiare, con cui ci siamo sostenuti, siamo impazziti (qualcuno più di qualcun'altro). Un grazie quindi a Rachele, Bruno, Denny, Guido, Gioele e Giuseppe per la loro compagnia quotidiana.
Ad maiora.

Sommario

Questo lavoro di tesi è stato svolto con l'obiettivo di studiare e testare l'utilizzo e il funzionamento di fibre ottiche come sensori per misurazioni di deformazione, variazioni di temperatura o pressione. Grazie alle apparecchiature presenti presso il *Laboratorio PhotoNext* del *Dipartimento di Ingegneria Meccanica ed Aerospaziale* del nostro *Politecnico di Torino* è stato infatti possibile allestire un banco prova e svolgere i test necessari a verificare e analizzare le variazioni di lunghezze d'onda misurate dal sensore *Fiber Bragg Gratings (FBG)* installato nella fibra, sotto particolari condizioni. L'obiettivo principale di questo lavoro di tesi è stato infatti, partendo dai risultati ottenuti in altri lavori di tesi precedentemente svolti (cfr. [1]), quello di utilizzare nuove apparecchiature per sperimentare la ripetibilità dei test precedemente svolti. In questo modo dunque è stato possibile automatizzare suddetti test e svolgere un numero molto più elevato di prove, al fine di collaudare la risposta della fibra sotto determinate tensioni, con determinate condizioni di temperatura. E' noto infatti, grazie alle recenti scoperte tecnologiche, che le fibre ottiche possono essere utilizzate in svariati modi, oltre che semplicemente per il trasferimento dati. Grazie alle loro caratteristiche di leggerezza e piccolissimi ingombri, al fatto che non necessitano di un'alimentazione esterna e che sono immuni ai disturbi elettromagnetici, si prestano infatti come ottimi elementi per poter realizzare innovativi sensori da installare a bordo di velivoli, sia in campo aeronautico che spaziale.

Summary

This thesis work has been conducted in order to study and test the functioning of the optical fibers as sensors. They can be used in fact to measure strain, temperature and pressure variations. Thanks to the equipments located in the *PhotoNext Laboratory*, into the *Mechanical and Aerospace Department* of our *Politecnico di Torino*, it has been possible to prepare a particular test bench. Thanks to it, we performed all the tests, verifying and analysing the wavelength variations. These measurements have been read through the *Fiber Bragg Gratings (FBG)* installed into the core of the optical fiber. So the objective of this thesis work consists, starting from other tests conducted in previous thesis work (see [1]), in using new equipments to make the tests automatic. Thanks to the substantial amount of measurements obtained in this way, we have been able to analyse the response of the fiber to particular stresses, with particular temperature conditions.
Because of recent scientific advances, it is known that optical fibers can be used in several ways and not just for data transmissions. They result to be very useful thanks to their low weight and dimensions. Moreover they don't need external power supply and they are immune to all electromagnetic disturbances. All these advantages make them so good to be used as sensors to be installed on-board, both in aeronautics and space.

Contents

List of Figures

List of Tables

Chapter 1

Introduction

In aerospace field, sensors has always been very important to guarantee optimum operation of the on-board equipments and to ensure high safety to every single mission, both in aeronautics and space. For these and a lot of other reasons, these sensors must to be very reliable, and - such as everything in our field - they should be as small and light as possible.

Hence, the need to use optical fibers as sensors. In this case they are able to measure temperature, strain and pressure variations. Nowadays, optical fibers are used in a lot of daily applications, from home furnishings to medicine. They are also used in important engineering fields, such as Telecommunication or Civil engineer. Uses of optical fibers for data transmission is very well known, thanks to their innovative characteristics. These fibers in fact are immune to electromagnetic interferences and they have high temperature resistance, so they can be used without problems in different adverse environments.

1.1 Thesis objectives

The objective of this thesis work is to test and verify the possibility of using optical fibers as sensors, in order to improve reliability of sensors and make them smaller and lighter. According to recent studies, in fact, it is possible to apply a small "change" in the fiber to permit you to use it like a normal sensor. As we will see in detail in the following chapters, in the core of the fiber a very small variation of the refractive index is made, in order to reflect a specific wavelength (*Bragg's Wave Length*). We are talking about *Optical Fiber Sensor (OFS)* and in particular way, we used *Fiber Bragg Gratings (FBG)*. In fact there are different types of OFS, but the FBG are ones particularly suitable to measurements in terms of strain, temperature and pressure. In any case, the use of fibers as sensors guarantees them to exploit all their positive characteristics described above, minimizing both dimensions and weight.

So, during our own work, starting from other tests conducted in previous thesis work (see [1]), we use new equipments to make the tests automatic. Thanks to the substantial amount of measurements obtained in this way, we have been able to analyse the response of the fiber to particular stresses, with particular temperature and ambient conditions. The most important objective is to understand how much these fibers are able to give us coherent and acceptable values when they are subjected to repetitive tests.

1.2 Thesis structure

For the convenience of the reader, we will summarise in this paragraph the structure of the thesis, considering all single chapter, starting from second for obvious reasons. The thesis counts 5 chapters, in which all characteristics of the fiber and how all tests have been performed are described.

The second chapter, titled *Optical Fibers and Fiber Bragg Gratings*, is useful to understand in detail how the *Optical Fiber Sensor (OFS)* installed into an optical fiber works. So we can identify two parts: the first one is focused on the optical fibers, the different types existing and their structure. The second one is focused on the Bragg, how it works and which physical laws allow us to use it.

Design of the test bench is the third chapter. Here it's possible to understand how all the system used to do the tests has been created. Even in this chapter we can identify two different parts: the first one is based on all the equipments and the hardware installed on the breadboard. The second one is centred about how to use them: it's described which software are used and how they work.

The fourth chapter is *Tests and Results*: it contains the most important part of the studies conducted. It explains in detail how the tests have been performed, which is the path followed and all the quantities measured. Then an important analysis of data collected has been conducted, in order to illustrate the response of the optical fiber to the stress imposed. An important part of this chapter contains the effects of external elements and describes how they can change the behaviour of the fiber.

The last chapter is titled *Conclusions and Future work*. Here it is possible to read the final considerations and observations about the results extracted from the previous chapter. The second part of this chapter is focused on hypothetical future developments, starting from the work done during this thesis.

At the end, there are two appendices. The first one is about a few tests developed at the end of the entire campaign described in the *chapter 4*. These tests have been performed using a different path, obtained reversing the previous one. It has the objective to demonstrate that the response of the optical fiber does not change. The second appendix describes a related work, executed by *Team Icarus*, in order to verify the relation between the wavelength and the temperature also in the static case.

Chapter 2

Optical Fibers and Fiber Bragg Gratings

Nowadays, optical fibers are more and more used, particularly in different fields of engineering. As mentioned previously, these fibers are very employed because of their innovative characteristics, such as:

- the ability to transfer big data with high data rate (broadband) and even for long distances;
- their immunity to every type of Electromagnetic Interference;
- low attenuation of the carried signal, instead of the long distance;
- high temperature resistance and chemical stability, especially in the case of glass fibers.

To understand better how the *Bragg gratings* work, an important detailed analysis of the *Optical Fibers* is necessary.

2.1 Optical Fibers'structure and characteristics

Starting from the beginning, we have to consider that these elements work in three bands of the electromagnetic spectrum: infrared, visible and ultraviolet (wavelength between 10^{-3} m and 10^{-8} m). Every single fiber is constituted from a *core*, and an outer part, called *cladding*. Both these "cylinders" are obviously coaxial, and each one has its particular index refraction n.

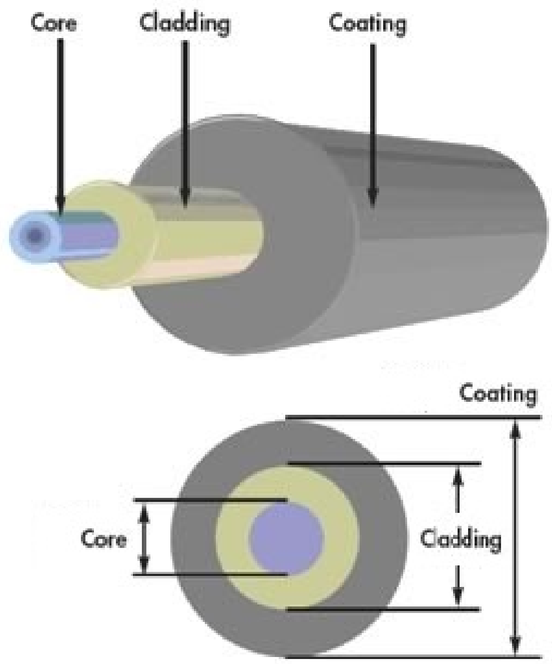

Figure 2.1: Optical Fiber: example of internal structure

As it's possible to see in the previous picture, both (core and cladding) are protected by an external coating. The material of the fibers is often a dielectric material, transparent to light. So they can be realized in glass, molten silicon or even plastic; obviously material's choice is related to the fiber's application. For example, plastic optical fibers are used in application with short distances, because of their high attenuation. On the other hand, glass fibers are best for long distance applications, and it is possible to increase or reduce their refractive index using particular chemical composite (such as German dioxide *(GeO_2)*, Aluminium oxide*(Al_2O_3)*, Titanium dioxide*(TiO_2)*). With these elements it's possible to change both refractive indexes of the core and cladding.

There are various type of optical fibers, depending on the modes of light propagation or on the refractive index. In particular, in the first classification we can recognize two types of optical fiber:

- *single-mode*: their diameter of the core is about 10 μm;
- *multi-mode*: their diameter of the core is 50 μm or more.

This classification comes from the fact that a core with larger diameter can use more than one mode of the light wave to pass on. As we saw for the materials, even in this case, the choice depends on application. A fiber with a thiner core in fact, is used in cases in which is necessary an high sensitivity (like for strain measurements). The second types, instead, are used when a rapid response to disturbances is requested. In the figure below we can observe the different diameter of the two cores:

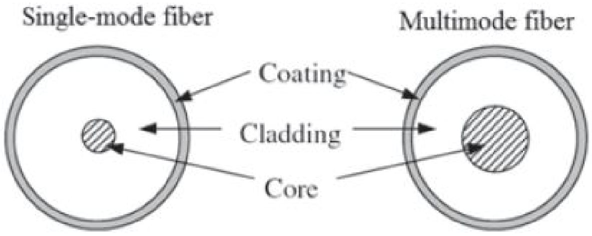

Figure 2.2: Example of different cores: *single-mode* and *multi-mode* fibers

.

Another type of classification depends on the refractive index, as mentioned previously. In this case we recognize:

- *Step index* optical fibers;
- *Graded index* optical fibers.

In the first one, both core and cladding have constant and uniform refractive indexes, but different from each other. For this reason, at the interface core-cladding we assist to a drastic reflective index change. In the second one, only refractive index of the cladding is uniform and constant; on the other hand the core has an index that changes with an almost parabolic trend. It has its minimum value along the interface between core and cladding and it reaches its maximum value along the axis of the fiber. It's possible to observe both these classifications in the following figure:

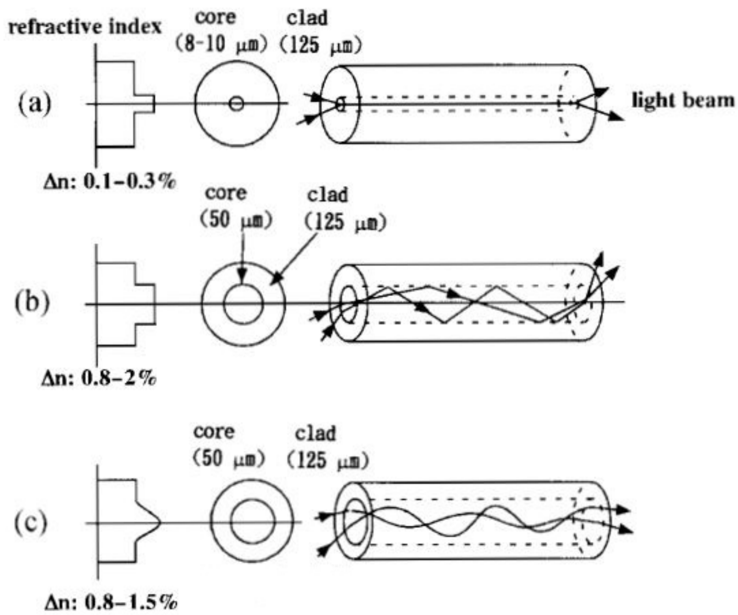

Figure 2.3: Example of wave light propagation: (a)*single-mode*; (b)*multi-mode* with *step index*; (c)*multi-mode* with *graded index* [2]

2.2 Propagation of the light

As everything in physics, propagation of the light (all confined within the fiber) into the optical fibers follows *Snell's law*:

$$n_1 sin(\theta_i) = n_2 sin(\theta_r)$$

During all this part, we will refer to the *incidence angle* with the subscript "i" and to the *refractive angle* with the subscript "r".

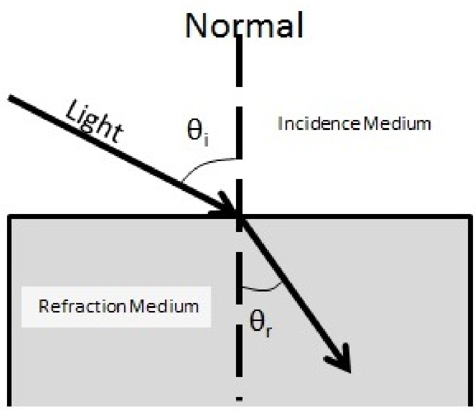

Figure 2.4: Example of wave light propagation: *Snell's law*

To better understand how this law works, we remember that the core and the cladding have different reflective index (here indicated respectively with n_1 and n_2) and in particular it's necessary that the refractive index of the core is higher than refractive index of the cladding. This characteristic is the basis of the *Total Internal Reflective* law: the light is always confined within the fiber just in case this rule is verified. We have to underline that the refractive index is simply calculated with the following equation:

$$n = c/v$$

in which c is the speed of the light propagation in vacuum and v is the speed of light propagation in the material to which it refers.

In order to guarantee that the light propagates into the core's fiber, the incidence angle must to be higher than the *Critical angle*, expressed by the following formula:

$$\theta = arcsin(n_2/n_1)$$

This condition is necessary because beyond this angle, all the light will be totally reflected and the light will stay into the fiber. This critical angle is reached when the refractive angle mentioned above is $\theta_r = 90°$. So, when a ray of light incises the optical fiber with an angle higher than the critical angle (or even equal) it does the total reflection, so it stays into the fiber. To guarantee this phenomenon the ray has to incises the fiber within an acceptance cone, identified in the figure below whit the letter "i".

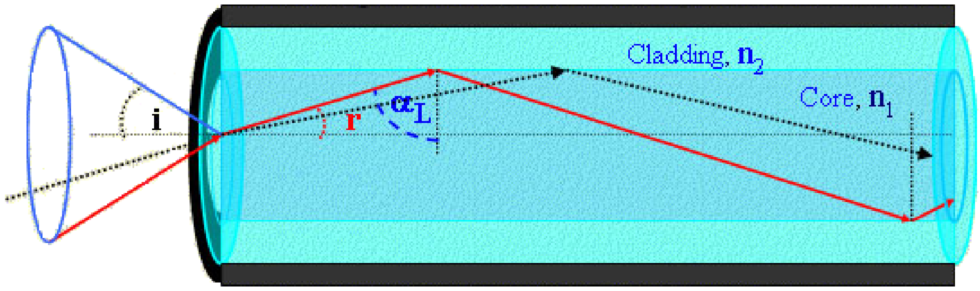

Figure 2.5: Example of wave light propagation in the optical fiber

Starting from now, we will refer to this angle with α_{max} and we proceed to calculate its amplitude, starting from the Snell's law. We are considering first of all the interface between the cladding and the external medium (usually air), indicating its refractive index with n_0:

$$n_0 sin(\alpha_{max}) = n_1 sin(\frac{\pi}{2} - \theta)$$

that can be rewrite as:

$$sin(\alpha_{max}) = \frac{n_1}{n_0} cos(\theta)$$

So we can obtain

$$sin(\alpha_{max}) = \frac{\sqrt{n_1^2 - n_2^2}}{n_0}$$

.

2.3 Structure of the FBG and its characteristics

As mentioned above, the types of *Optical Fiber Sensor (OFS)* we used are *Fiber Bragg Gratings (FBG)*. It's easy to understand how important are, in our field, sensors. They have to be reliable, light and as small as possible. The FBG sensors perform a new frontier in sensor technology, and thanks to their advantages, they are used in many field of engineering. Another particular characteristic is that they don't need external electric power source. So in this paragraph we want to explain how they work and their physical principles.

With regard to the FBG's so, they consist in a particular (and very small) variation of the refractive index in the fiber's core. This "change" is made by literally writing in the fiber's core a variation of the refractive index: in this way a short portion of the fiber (a few millimeters) is able to reflects specific wavelengths and the remaining part is transmitted. A lot of methods have been invented to write the FBGs into the fiber's core, using for example a periodic variation of the refractive index or a non-periodic variation, as we can see in the figure below:

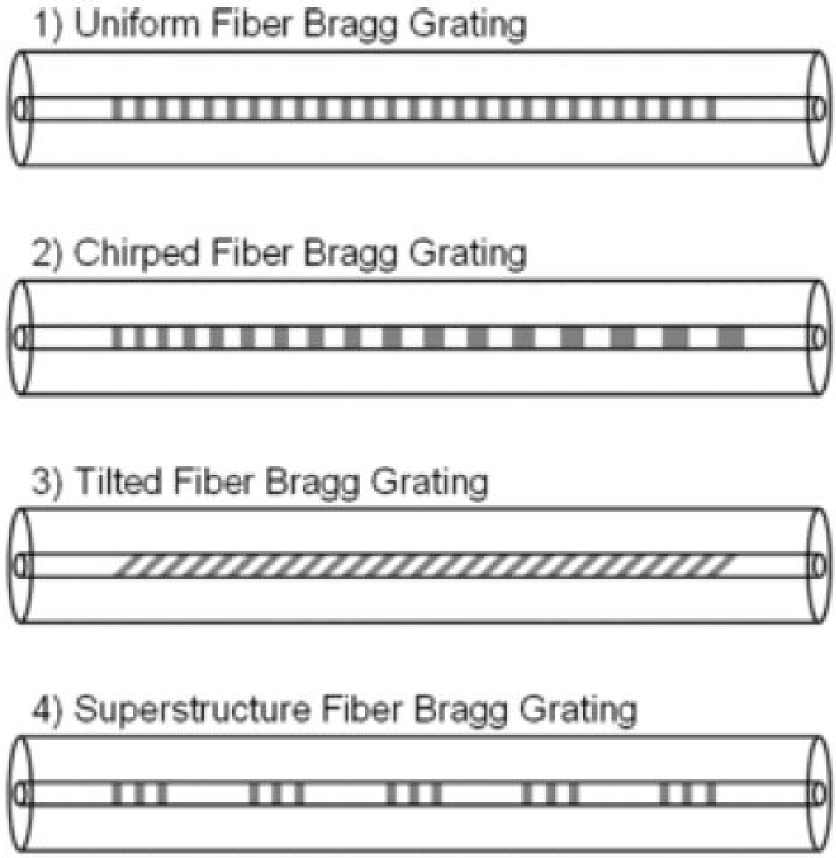

Figure 2.6: Type of FBGs: (a) *Uniform FBG*; (b)*Chirped FBG*; (c) *Tilted FBG*; (d)*Superstructure FBG* [3]

Obviously, the choice on the type of FBG depends on the applications. For example, typology (b) (*chirped*) is used for antenna systems, because its structure permits to change the reflected wavelength along the Bragg. On the other hand, the type with *tilted FBG* has a change of the refractive index at an inclination to the optical axis, that modify the reflected wavelength.

In our case, the fibers used were prepared with a periodic (constant) variation of the refractive index, as shown in figure 2.6 (a). So, the physical formula that characterize our FBGs is:

$$\lambda_B = 2n\Lambda$$

in which we called λ_B the wavelength of the Bragg written in the optical fiber. The term n represents the effective index of the grating, and the the term Λ is the period with which the grating has been written. When these sensors are used is necessary to apply a shift of this wavelength:

$$\Delta\lambda_B = \lambda_B[(\alpha_t + \zeta_t)\Delta T + (1 - P_e)\epsilon]$$

In the previous equation, the terms α_t and ζ_t are respectively the thermal expansion and thermo-optic coefficients of the fiber, meanwhile the term P_e is a photo-elasticity constant. The terms ΔT and ϵ represent, obviously, the temperature variation and the strain. This shift of wavelength is necessary when both temperature and strain contribute in the mechanical or thermic tests. Generally, the behaviour of a periodic FBG sensor, as in the optical fibers used for our tests, is like the one shown in the figure below:

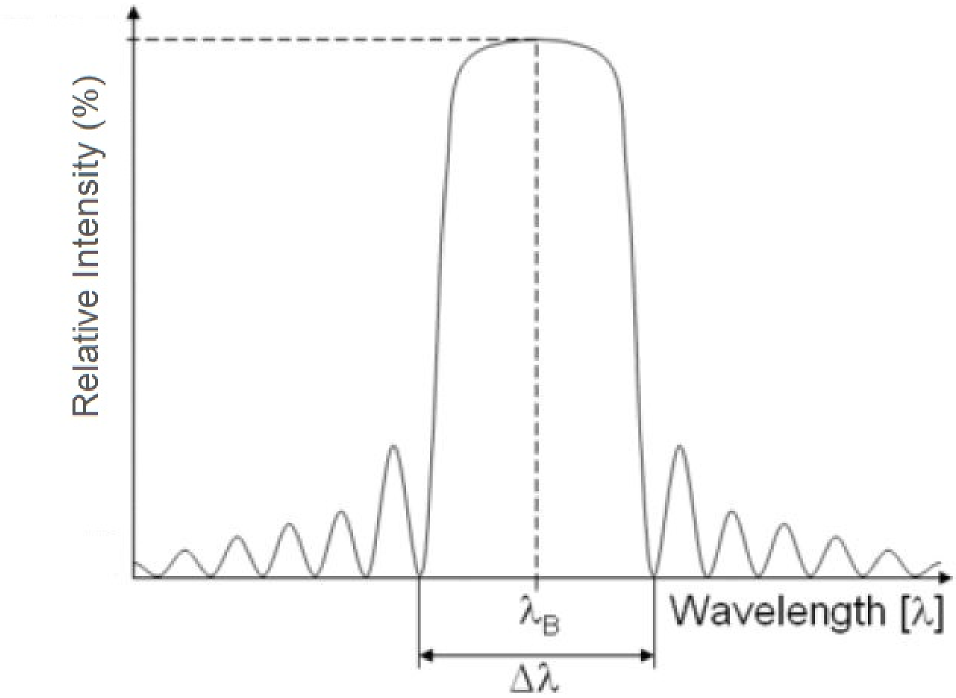

Figure 2.7: Example of relative intensity as a function of wavelength [3]

We can observe in this picture the principal wavelength read by the Bragg in the optical fiber.There are other secondary wavelengths which represent the noise.

Another important advantage of this new kind of sensors is the possibility to create a single optical fiber with a lot of FBGs. In fact we can write two or more FBGs (even with different λ_B) in a given fiber, or we can "create" our own fiber using a particular process of splicing. With this method is possible to divide two FBGs, each belonging to a fiber, and "paste" them into a single fiber. Obviously, even in this case, we can produce a fiber with two or more FBGs. In any case, we have to remove the external coating of the fiber, and at the end of the process is necessary to recreating it, re-coating the fiber. We can understand that it is a cheap and fast method to obtain a fiber with a certain number of FBGs, strategically positioned. On the other hand it is a delicate process, that requires specific machinery to ensure optimal results and to avoid to damage the optical fiber.

2.4 Disadvantages

As everything, the use of this new technology has a few advantages, necessarily followed by some disadvantages. First of all, we have to consider the economic factor: as mentioned before, they don't need external (electric) power, but in any case these elements are not cheap, because of the equipments necessary to create the FBG inside the fiber. We should taking into account, also, all the machinery necessary to read informations transmitted by the fiber.

Moreover, these optical fibers are very breakable, especially during the assembly of the test bench phase, or for example, during the splicing operation. So they results a little bit difficult to install and if this operation is not executed in a correct way, inaccurate results can be obtained. For this reasons a lot of studies have been done in order to choose the better way to install it to minimize losses and the others phenomena of viscous nature.

So we can summarise for the convenience of the reader these disadvantages related to the optical fibers:

- the difficult to install them: a bad installation can damage the optical fibers and a high curve radius can increase losses;
- the influences of all the external factors. We remember that, in order to avoid interferences of vibrations or other effects, apposite breadboards have been used;
- the economic factor: the equipments necessary to assembly the test bench and all the interrogation system are not cheap.

In the following chapters we will see the chosen design, the resin used to fix it and obviously the type of optical fiber with which tests were performed (in terms of materials and internal structure).

Chapter 3

Design of the Test Bench

In this chapter we will see how the test bench has been planned and the equipments used and created *ad hoc* to perform all the tests. Moreover, we will explain the hardware installed to guarantee the correct method of operating and the software necessary to run the tests.

3.1 The fiber and the breadboard

First of all, it's necessary to specify which optical fiber has been used to execute the tests. We explained in the previous chapter all the fiber's characteristics, the different materials and types of Bragg.

Thanks to the *Femto Fiber Tec* that gave us all the fibers necessary to our work (through the ISMB), the optical fiber used to execute these particular tests has the the following characteristics:

- *coating material*: polyimide;
- *type of FBG*: periodic variation;
- *center wavelength*: $\lambda_0 = 1555.06\ nm$.

Focusing on the dimensions that characterize our optical fiber:

Element	**Dimension**
Total length	2.00 m
Position of the FBG	1.00 m
FBG length	3.2 mm
Core diameter	9.8 μm
Cladding diameter	125 μm

Table 3.1: Summarise of physical characteristics of our optical fiber

Now we can see, showing some pictures, how the test bench has been prepared, starting from an optical enclosure realised with plexiglass panels.

Figure 3.1: Optical enclosure *(Copyright 1999-2018 Thorlabs, Inc.)* [1]

This enclosure has been chosen because of the need to isolate the fiber from external noise and wind. In fact it's difficult to select a start wavelength to execute tests if an external noise or wind shifts it. This factor can reduce the accuracy of the tests, hence to choice to protect the fiber with this equipment. It's right to specify that the backward panel has been drilled in order to allow the connectors to be passed through and to be connected to the interrogator.

In order to make the tests as accurate as possible, this enclosure is positioned on another breadboard which has a particular anti-vibration system, that guarantees isolation from vibrations coming from outside the building (for example the presence of urban traffic).

In the following paragraphs we will discuss how the fiber has been mounted in this enclosure, showing in details all the devices used.

3.2 The hardware

Firstly, it's convenient to make a list of the equipment necessary to assembly all the system. Taking into account that the breadboard's base is in Aluminium and it has *M6* threaded holes separated from each other of 25 *mm*, we used the following equipments to fix the fiber on it. In particular, two elements are sufficient in one end of the fiber:

- Bottom base, directly mounted on the breadboard, *in Aluminium*
- Upper base, mounted on the previous element, *in PLA*

We can show these two elements, mounted on the breadboard in the picture below:

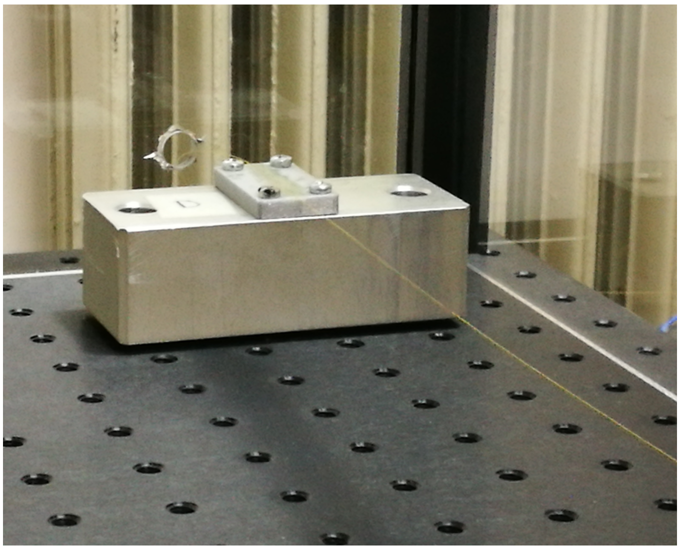

Figure 3.2: One end of the optical fiber, fixed on the breadboard

To fix the optical fiber on the other end, three elements have been engaged:

- Bottom base, directly mounted on the breadboard, *in PLA*
- The electric micro-translation, fixed on the previous element
- Upper base, directly mounted on the micro-traslation, *in PLA*

These three elements, fixed on the breadboard are shown in the following picture:

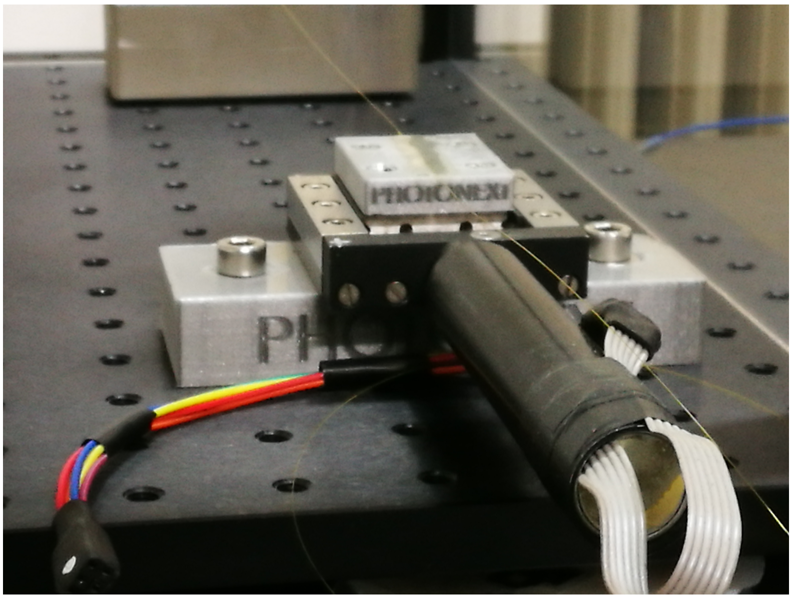

Figure 3.3: The other end of the optical fiber, fixed on the breadboard with its micro-translation

The fiber has been fixed on both ends directly on the upper plates in PLA, using specifically an epoxy resin. Obviously, these elements have been mounted on the breadboard in order to assure an horizontal position to the fiber and a specific length of $L_0 = 228{,}94\ mm$. The choice about this particular length and the use of the epoxy resin is justified by a set of studies carried out in previous thesis work (see [1]), in order to reduce losses caused by some phenomena of viscous nature. About the process to glue the fiber on the plates, it's better to underline that it is a delicate process, so it has been realized very carefully. During this phase in fact, it's necessary to use special mixers for the glue (Araldite, as mentioned above, is a bi component resin), to clean very well both the fiber and the plate and to pay a lot of attention to some details:

- the fiber must to be in the centre of the plate, on both ends;
- the fiber should be as tight as possible;
- the glue layer must be as thin as possible.

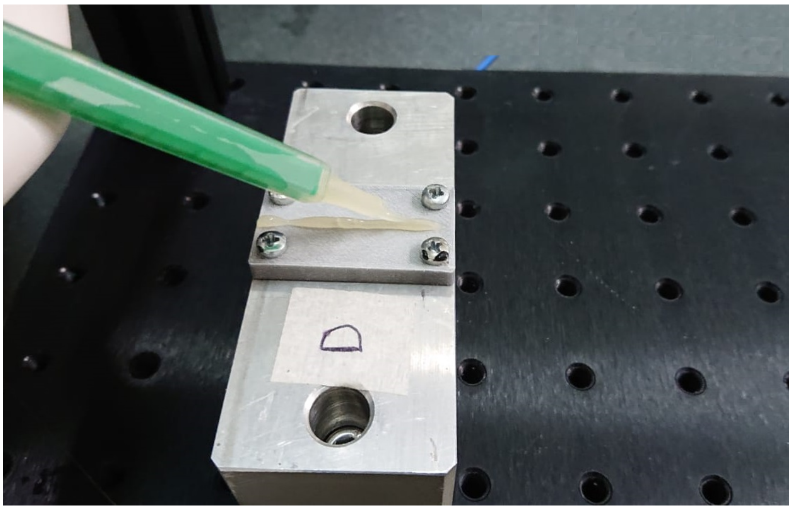

Figure 3.4: Gluing phase: Araldite with special mixer

The elements in *PLA material* have been produced with a 3D-printer, with the support of a CAD program. After accurate measurements performed on the breadboard and on the elements necessary to execute the tests, they have been modeled as shown in the figures below:

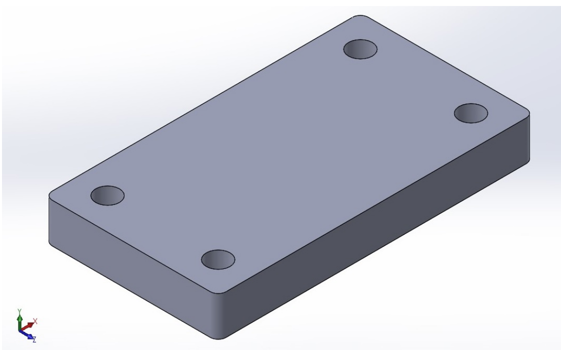

Figure 3.5: Upper base, mounted on the Aluminium base

This first base is just a rectangular base, with four through holes that permit to fix it on the bottom base, in Aluminium, directly mounted on the breadboard. The fiber is glued on this base, on its centre (cf. 3.4).

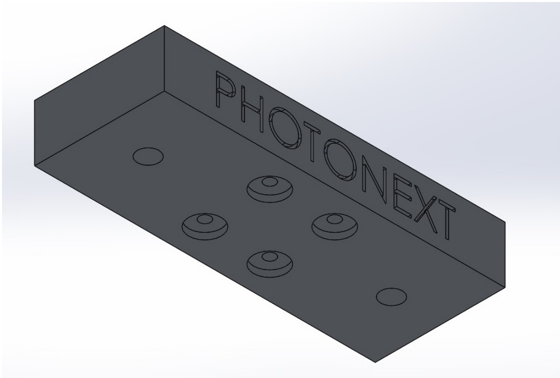

Figure 3.6: Bottom base, mounted on the breadboard, designed to fix the micro-translation

This second base is used on the other end of the fiber. In particular way, we designed this PLA base in order to be able to fix the micro-translation on the breadboard. In fact their respective holes did not match, so we have been forced to create this equipment. It's possible to see in the figure above that it has been designed with two external through holes, necessary to hold the system on the breadboard. But first of all, you have to hold the micro-translation on this plate, using the other four through holes on the centre. As you can notice, they are countersunk holes on the lower face of the plate, in order to permit to place it on the breadboard. To better understand its geometry, we display two other pictures:

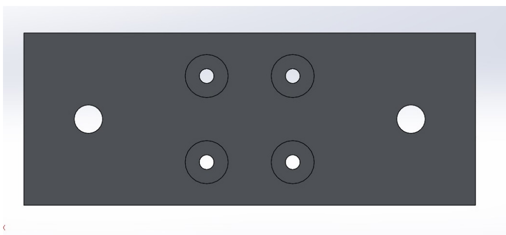

(a) *Bottom view*

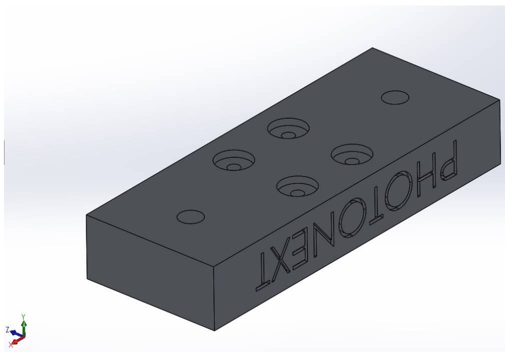

(b) *3D rotated view*

Figure 3.7: Different views of the previous plate

At the end, we have to describe the upper plate, fixed on the micro-translation, previous hold on the bigger base (cf. 3.6):

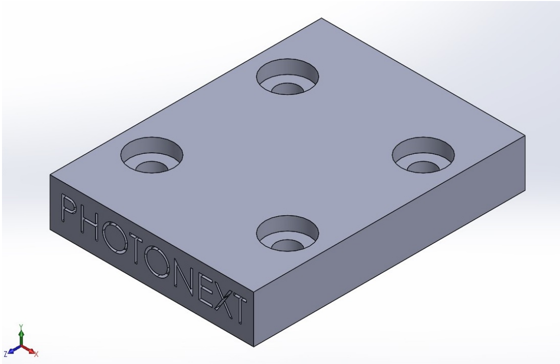

Figure 3.8: Upper plate, fixed on the micro-translation

Even in this plate, like in the previous one, four countersunk holes have been realized. This plate has the important role to move itself with the micro-translation, in order to guarantee the increasing and decreasing of the optical fiber's stress. (cf. 3.3)

For the convenience of the reader, we can summarise all the characteristics of the test bench realized *ad hoc* to perform this tests:

Element	**Characteristics**
Coating material	Polyimide
Support's materials	Aluminium
	PLA
Type of glue	Epoxy Resin: Araldite
Effective length	$L_0 = 228.94\ mm$

Table 3.2: Summarise of characteristics of the test bench

So, at the beginning of the tests, the breadboard is composed like in the pictures below:

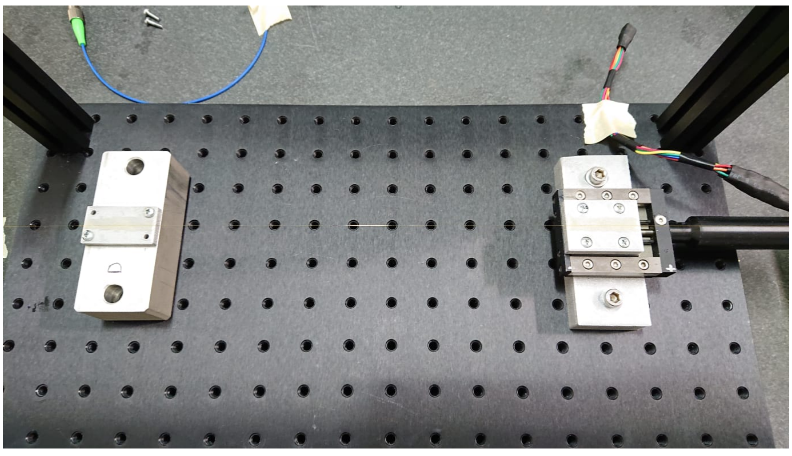

Figure 3.9: Top view of the total system

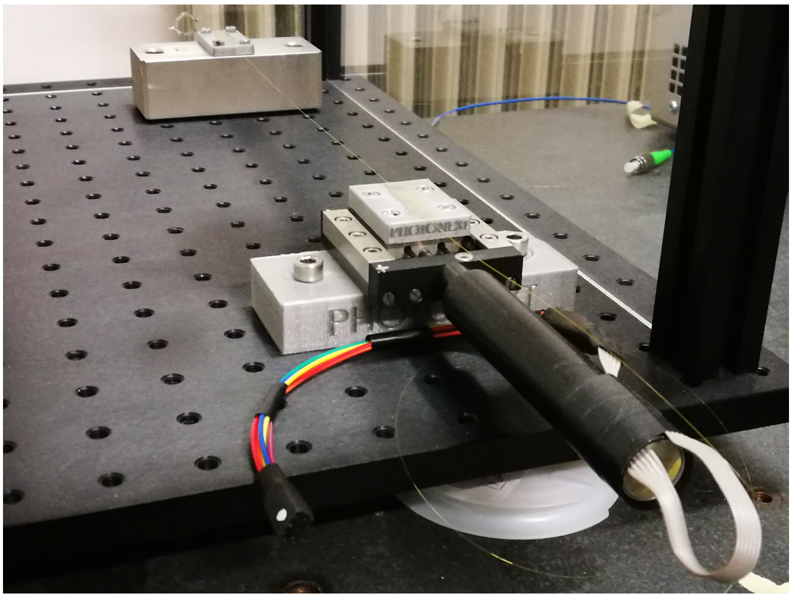

Figure 3.10: Assembly of the total system

So, we can describe rapidly how the micro-translation works. It is a "TMS-16" servo motorized micro-translation, with a 3922 *steps* TTL magnetic encoder. Moreover it has a 8V brushed DC motoreductor with the following characteristics:

Element	**Dimension**
Stroke	16 mm
Speed	0.2 mm/s
Acceleration	0.2 $\mu mm/s^2$
Resolution	1 μm
Accuracy	± 3 μm

Table 3.3: Characteristics of the micro-translation

Its position control system is constituted by a control loop in which both an integrative and a derivative loop have been inserted. Practically, it is a PID controller, with a notch-filter; they are also saturated, in order to avoid overflows. Also an H-bridge is necessary, in order to allow to invert the polarity of the DC motor, so the micro-translation can be moved in both, positive and negative, positions. In particular it is designed to provide bidirectional drive current up to 1 *Ampere* and with voltages from 4.5 V to 36 V. At the end, 10 nF capacitors between the encoder pins and the ground have been installed, in order to avoid false-contacts. You can see this circuit in the picture below:

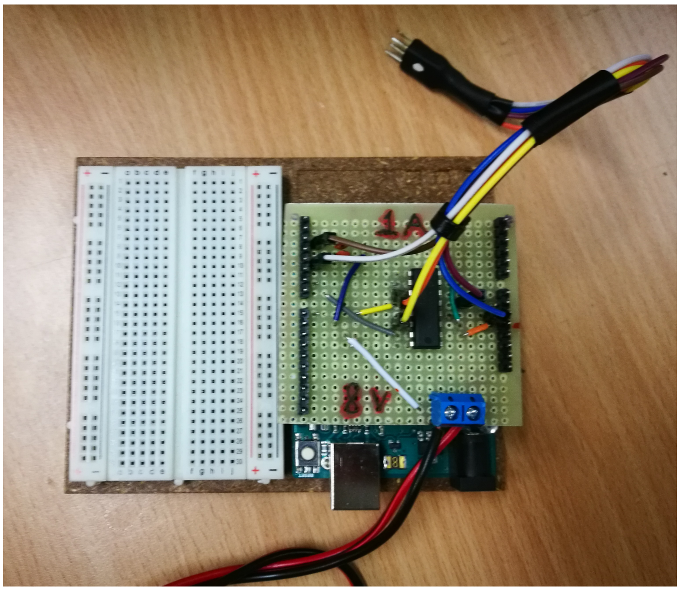

Figure 3.11: Circuit created *ad hoc* for the micro-translation

Obviously, as you can see, this circuit need to be connected with an ARDUINO platform (described below). At the end of this paragraph, a list of the other hardware elements necessary to perform the tests will be done. Their functioning will be broadly discussed in the next paragraph. These elements are:

- ARDUINO platform with special circuit, made *ad hoc* to control the micro-translation

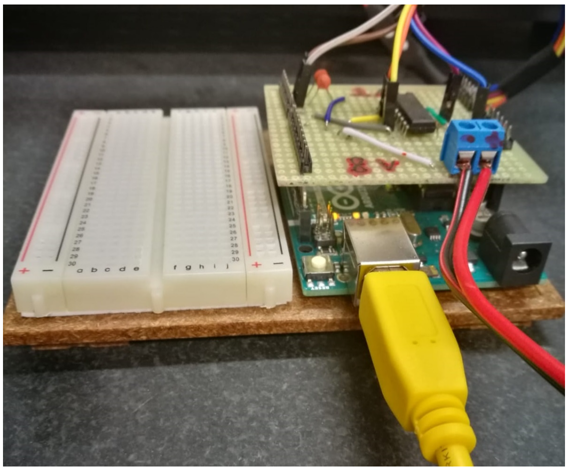

Figure 3.12: ARDUINO platform, with its own electronic circuit

- Dynamic FBG interrogator *“Smart Scan”* to read wavelength of the optical fiber

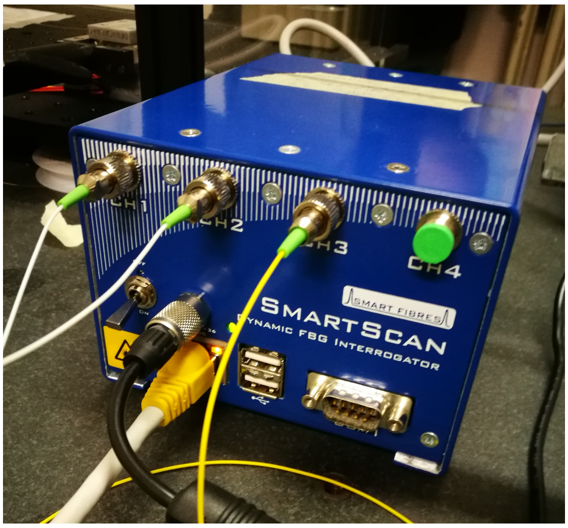

Figure 3.13: Dynamic FBG interrogator

- a stabilized power supply correctly set, to power the electric circuit and to guarantee the movement of the micro-translation

Figure 3.14: Stabilized power supply - *we used the second channel for logistic reasons*

About the stabilized power supply, its settings depend on the micro-translation, so the reason for the values used (5 $Volts$ and 1 *Ampere* as shown in the picture) will be discuss in the next paragraph.
So, just before to describe how these equipments work, it’s necessary to understand how they are connected to each other. We will use the graph below to better help the reader on this phase:

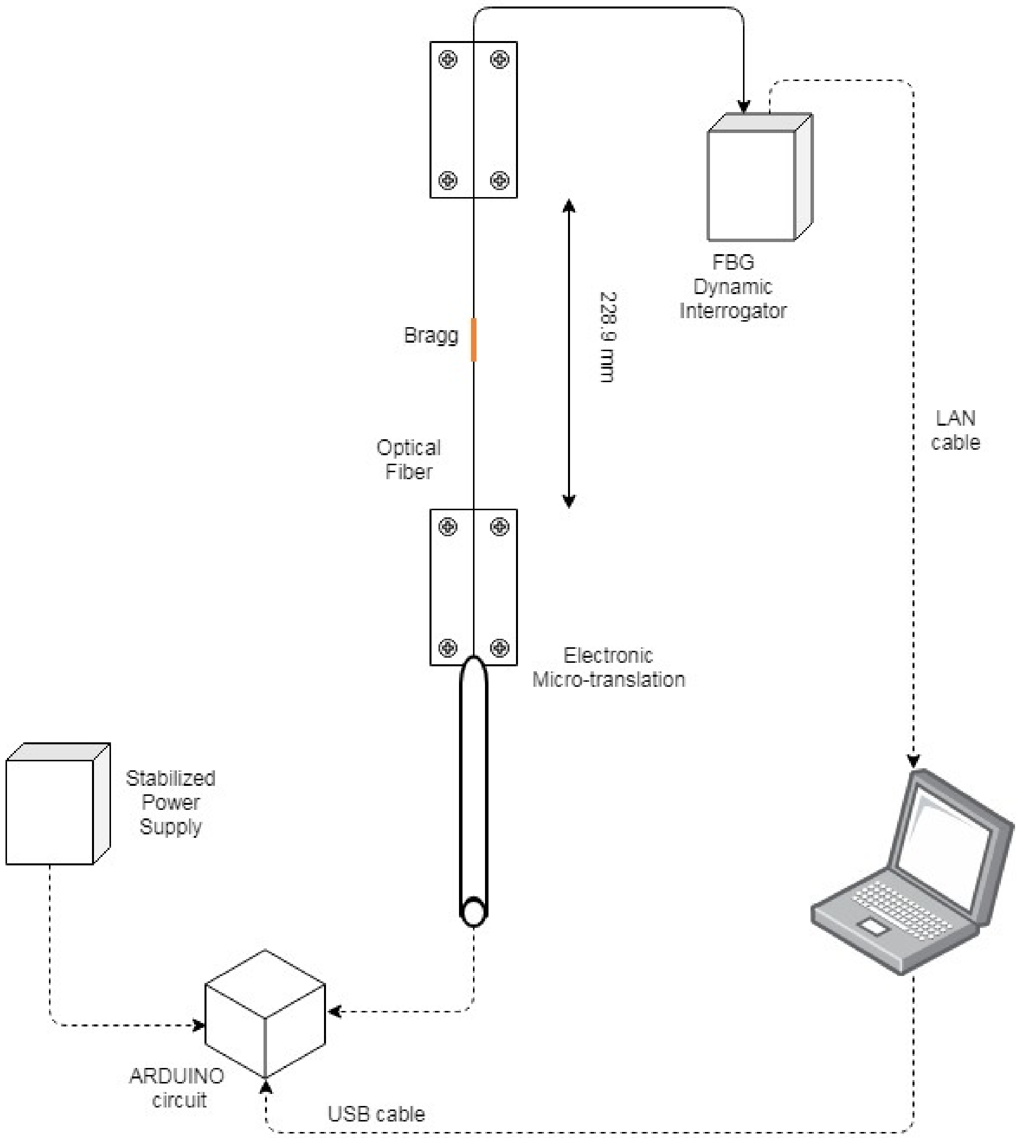

Figure 3.15: Graph of the equipments of the test bench: all the links

In this picture, the only continuous line represents the optical fiber, with its own FBG on its centre. All the other non-continuous lines are the physical connections. It's possible to see how the fiber is hold on the plates described previously and one of its ends (the upper, in this graph) is directly linked to the *Smart Scan - Dynamic FBG Interrogator*. It is connected to a Personal Computer via LAN, to permit us to read the value measured by the Bragg. Also the ARDUINO is connected with the PC, by a USB cable, to permit to command the movements of the micro-translation. To ensure the correct value of voltage and current, the stabilized power supply is connected to the ARDUINO, directly linked in turn with the micro-translation.

3.3 The software

In this paragraph we will see the software used to run tests. First of all we can summarise them in a rapid list:

- the ARDUINO software, to communicate with the electric micro-translation;
- a MATLAB script, to run the test designed automatically;
- the *SmartSoft SSI*, to read and save information of the Bragg;
- other MATLAB scripts, to process data collected.

3.3.1 ARDUINO Software

Communication with the electric micro-translation was not easy, because of its backward electronics. So an electric circuit has been created *ad hoc* (cf. 3.11) and an ARDUINO specific code was implemented. Thanks to this code, it's possible to control directly the micro-translation. From this, the need to use 5 $Volts$ to command it: in a first time we tried to use something more (8 $Volts$) but a problem occurred. With an elevate voltage value in fact, we transferred too much information in too little time with the risk that ARDUINO was not able to process them. We could obtain for this reason a wrong counting of the steps that it have to do and consequentially a wrong stress applied to the optical fiber. Hence the choice to use 5 $Volts$ united to a maximum value of current equal to 1 $Ampere$, dictated by the own electronics of the micro-translation.

So, after long and detailed appropriate studies, we have been able to know how many "steps" you need to impose to the micro-translation in order to obtain a movement of a turn of its internal screw:

$$1\ turn\ of\ screw = 0.5\ mm$$

$$1\ turn\ of\ screw = 3922\ steps$$

Known this information, it's simple to understand that, using the apposite code, we stabilized a serial communication between our personal computer and the ARDUINO, that manages in analogue mode (using the H-bridge previous described). In this way we have been able to choose (every single time) how many millimetres to move the micro-translation and then the plate. It's possible to move it both in positive and in negative positions, in order to stretch the fiber or release it. So we have been able to quantify, in terms of wavelength, the stress caused by a particular given movement.

3.3.2 MATLAB script

As mentioned before, the type of tests performed have been chosen on the basis of the previous thesis work (see [1]). These particular tests, as we will describe accurately in the following chapter, consist of a certain number of step commands. In particular, starting from a zero position, 10 *steps* of 0.05 *mm* will be done, in order to reach 0.5 *mm*, equal to a turn of the micro-translation's internal screw. At the end of these 10 *steps* the zero position is reached again, in order to start the second test.

To guarantee this particular path, the MATLAB script called *command.m* has been written. It permits to change easily all the quantities involved:

- the duration of every single step;
- the magnitude of every single step;
- the maximum magnitude to reach;
- the number of steps to command.

Thanks to this code, every time that the script is run, it communicate with the ARDUINO code previously described and it transfer the commands to the micro-translation, that executes them. When the script is run, it's possible to see in real time the micro-translation activity in a plotted graph that will be automatically saved in the script's directory as a ".jpg" picture:

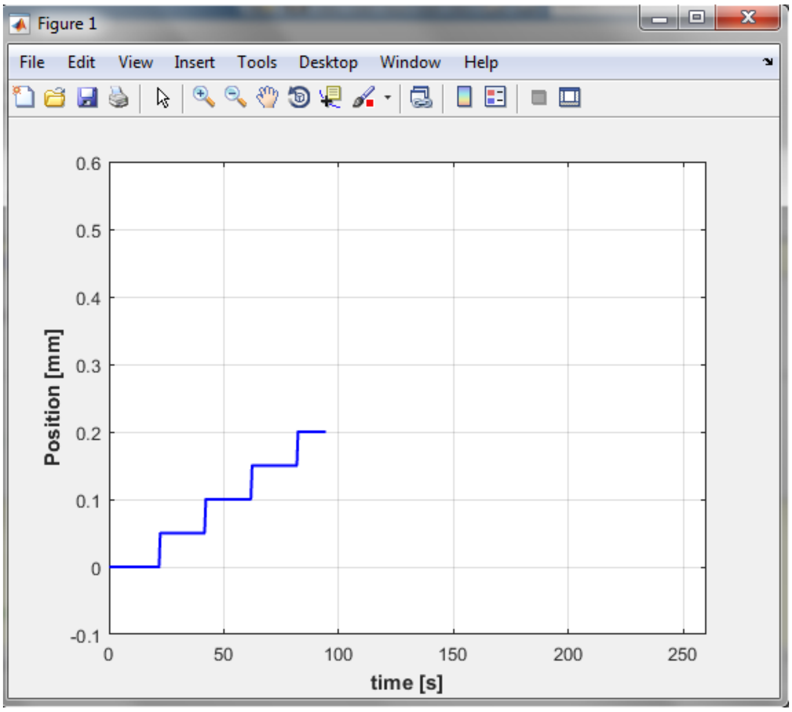

Figure 3.16: Micro-translation activity during a test

To process data collected from tests, other many MATLAB script will be necessary. These scripts will be useful to analyse data collected by the interrogator (with the software described in the following paragraph), because we were not able to analyse them correctly in real time. Starting from a ".log" file (that is a normal file text, given by the interrogator), it's easy to run the MATLAB script called

Post_processing_3_ 0.m. It requires the user intervention in order to set some parameters: it's necessary to communicate it the complete file name to load, then to select if the user wants to add comments. Moreover it's requested the type of analysis (standard or personalized) and to set some other parameters. In our case, as the reader will see in pictures reported in the following chapter, all the analyses are focused on the wavelength, so this characteristic will be the one that will be presented into the graphs. With this script was possible to analyse the strain too (if you have read information by the Bragg in this format). At the end, the script *fitting.m* is run, in order to compare values obtained by the test with theoretical values. It need a few modifies, depending on some characteristics used to perform the tests (for example the length of the fiber used). This MATLAB script produces a lot of graphs and some of them will be very important and relevant to our own analysis, as we will show in the following chapter. Both these last two scripts have undergone a minor change: an offset in time terms has been imposed. In this way, the first step perfectly correspond to the value of 10 *seconds* and all the other steps are obviously realigned in order to obtain graphically something more readable. In fact, starting the reading by the interrogator and running the *command.m* script to move the micro-translation, it was impossible to match times correctly.

3.3.3 SmartSoft SSI

This software permits us to read and save all the Bragg's information. It is possible to connect at the *Dynamic FBG Interrogator* even four optical fibers simultaneously, and each of them can have even a dozen Braggs. If the software is correctly installed and the interrogator correctly connected to the computer (and the pin of the optical fibers correctly inserted) it's possible to read in real time all the wavelengths of all the Braggs present, such as in the example below:

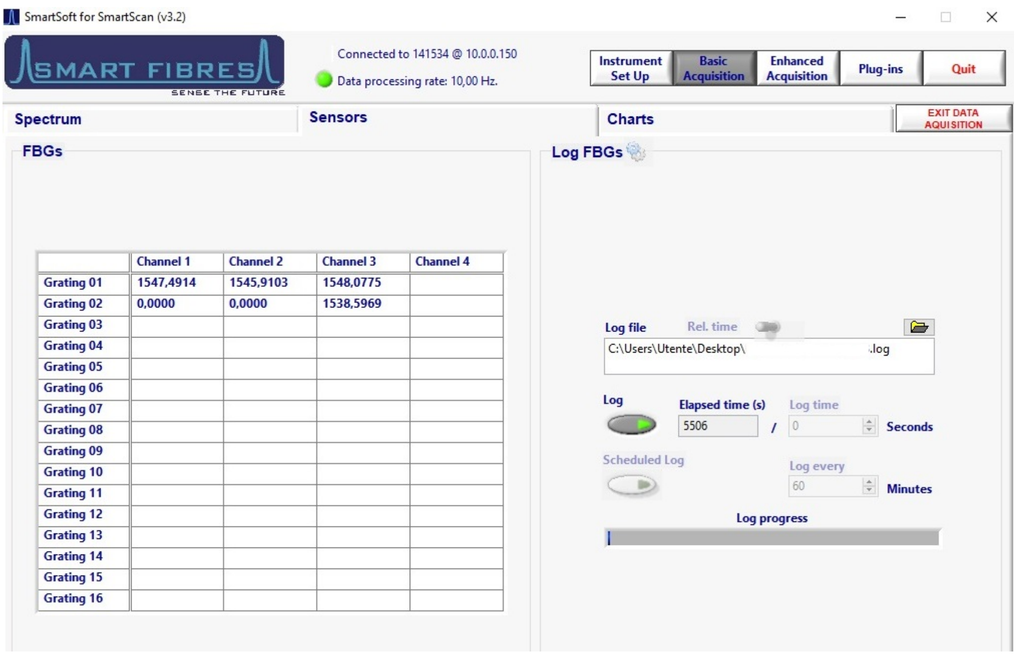

Figure 3.17: Example of the software SmartSoft

If you want, you can read even a lot of other information, such as strain conditions. In this particular case, our tests have been conducted on one single optical fiber, with just one Bragg sensor.

The most important use of this software is to save into a ".log" file (easily readable as a text file) all the information collected. First of all, you can see in real time the information read by the FBG, even in static or dynamic conditions. So, when the micro-translation starts to move, it's possible to save (and also to see in real time) all the wavelengths assumed by the optical fiber during all the test. The user can also choose in this part the sampling frequency, i.e. the time intervals between one capture and the following one. In our case this time is fixed to 0.1 *second*, so the files ".log" obtained are composed by only two columns: the first one (on the left) containing the time intervals and second one (on the right) containing the wavelength values in nano-meters.

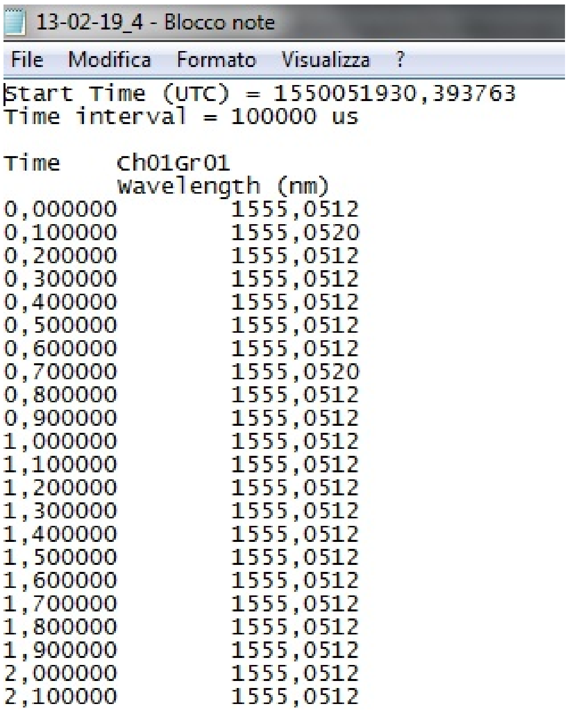
13-02-19_4 - Blocco note
File Modifica Formato Visualizza ?

```
Start Time (UTC) = 1550051930,393763
Time interval = 100000 us

Time     Ch01Gr01
         Wavelength (nm)
0,000000        1555,0512
0,100000        1555,0520
0,200000        1555,0512
0,300000        1555,0512
0,400000        1555,0512
0,500000        1555,0512
0,600000        1555,0512
0,700000        1555,0520
0,800000        1555,0512
0,900000        1555,0512
1,000000        1555,0512
1,100000        1555,0512
1,200000        1555,0512
1,300000        1555,0512
1,400000        1555,0512
1,500000        1555,0512
1,600000        1555,0512
1,700000        1555,0512
1,800000        1555,0512
1,900000        1555,0512
2,000000        1555,0512
2,100000        1555,0512
```

Figure 3.18: Example of the ".log" files

Chapter 4

Tests and Results

All this chapter is focused on the tests developed during the last months dedicated at this thesis work. So, to perform the tests we used the tests bench exactly composed as described in the previous chapter *("Design of the Test bench")*, such as both the hardware and the software.

First of all it's necessary to illustrate how the tests have been conducted, in order to better understand the results obtained. This thesis work in fact is based on a previous work, developed by *G. Candiano* (see [1]) in the same *PhotoNext Laboratory*. The substantial difference is about the micro-translation: we used an electrical one (instead the manual type used previously) in order to make the tests automatic and repeatable. During its own work, *G. Candiano* tested also the locking systems and the better length of the optical fiber to use to perform the tests in order to have results with an influence of the viscous phenomena as little as possible. Hence, in order to repeat that type of tests and to analyse the response of the Bragg when stressed several times, we chose the epoxy resin (instead the rubber into two aluminium plates) as glue for the locking system and to adopt the maximum length possible (228.94 *mm* - cf. 3.2). In fact, both these choices permit to reduce losses in precision caused by viscous phenomena, so they permit us to obtain results as reliable as possible.

So, focusing on the tests, they consist in one single type of measurements repeated a lot of times. The path is done considering 10 *step* commands, with an amplitude of 0.05 *mm* for each one and with a duration of 10 *seconds* given with a pause of other 10 *seconds* from the following one. In poor words, in every single test there are 10 *seconds* during which the micro-translation is moving, passing from a step to the following one, and the following 10 *seconds* during which it keeps the given position. So, into the ".log" files, all the movements are keeping in count, registering the information from the FBG every 0.1 *seconds*, but for the analysis executed on these data just the constant parts of the steps are relevant. To better understand how the tests work, we include a picture with the entire path used, starting from the *zero position* ending to 0.5 *mm*, at the end of the 10 *step* commands:

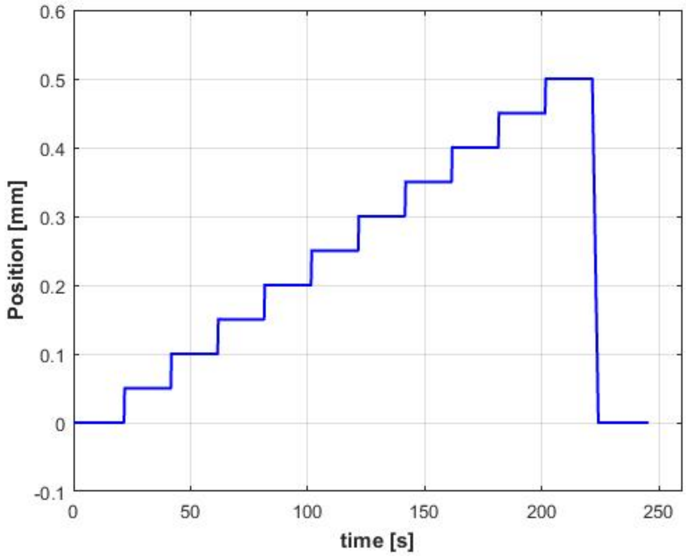

Figure 4.1: Real path followed during the tests

Obviously, as mentioned before the speed of the micro-translation is limited and it has its own inertia, so if you could zoom on the graph above you could see that the segment that it follows to go to one step to the following one is not perfectly vertical.

For the convenience of the reader, it's possible to see in the graph below the characteristics described above: in the picture the relevant part of the analysis (i.e. the 10 *seconds* of the constant part of every step) are signed in red.

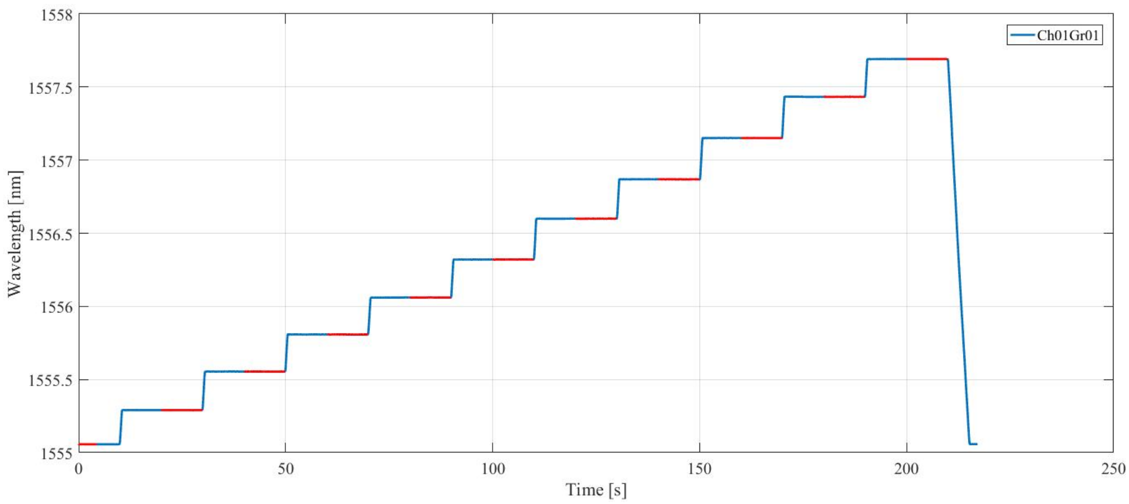

Figure 4.2: Example of tests performed with relevant data

It's easy to understand by the picture above, that at the end of every single test, the MATLAB script used to execute this path was written in order to force the micro-translation to return at the initial position, called for convenience *zero position*. So, considering a total length of the optical fiber of $L_0 = 228.94\ mm$

and a final length variation imposed of $\Delta L = 0.5\ mm$ we can calculate the strain:

$$\epsilon = \frac{\Delta L}{L_0} \simeq \frac{\Delta \lambda_B}{(1 - P_e)\lambda_B}$$

from which we obtain:

$$\epsilon = 2180\ \mu\epsilon$$

4.1 Preliminary work

From the experience gained during this period of thesis work, we understood that a specific and depth control was necessary. In particular way, the goodness both of the optical fiber and, even more, of the gluing needed to be verified and tested. So in this paragraph we will describe how we validated all the system, once the test bench was definitively assembled. Generally, we have performed some tests with particular paths (different from the one that is representative of this work) in order to understand if something does not work in the right way. As mentioned many times, a variety of phenomena could occur and they could invalidate tests.

First of all, the goodness of the gluing needed to be verified: it's possible to see the behaviour of the optical fiber to particular stresses and try to understand if the glue is collapsing or not. It's useful to underline that these tests have been conducted a few days after the gluing process, to ensure the glue drying process was completed. So, a few tests have been performed giving a step command of a complete turn of the internal screw of the micro-translation and this position has been kept for a long time (about 30 *minutes*):

$$1\ turn\ of\ screw = 0.5\ mm$$

We remember that this value is equal to 3922 *step* to command by the ARDUINO circuit to the micro-translation. To better understand how this type of test can be useful, the graph obtained processing data is reported below:

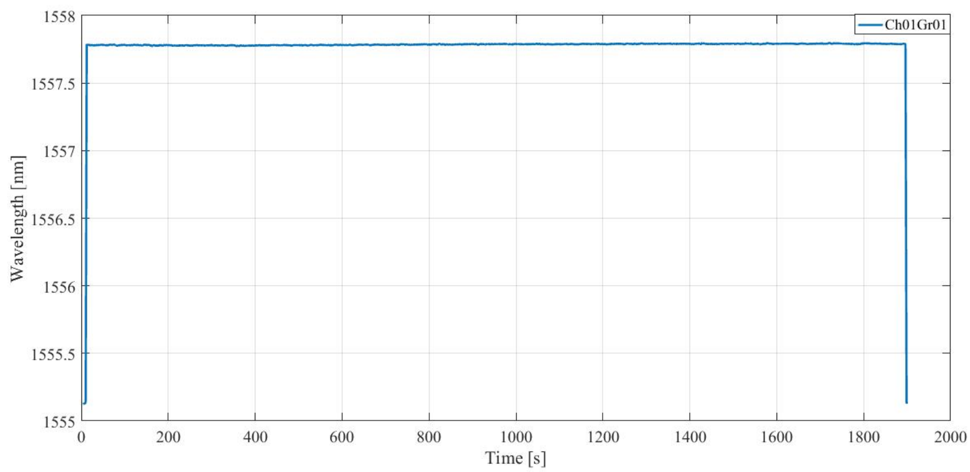

Figure 4.3: Step command kept for long time

Obviously, as it's possible to notice by this picture, the zero position is reached again at the end of the test. The important information that we obtain is strictly connected with the goodness of the gluing done. In fact, zooming on the constant part of the graph, it's easy to see that the position commanded is perfectly maintained (in terms of wavelength):

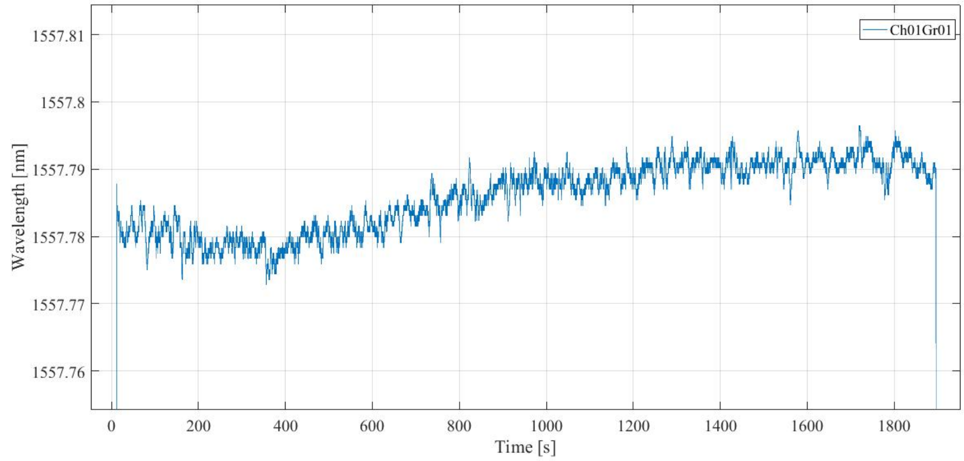

Figure 4.4: Zoom of the previous graph

In other words, once the micro-translation reaches the position, the information given by the Bragg does not change, even after a long time (here about 1800 *seconds*). It means that the glue is not collapsing, instead it is able to measure a small growth on the wavelength, probably caused by external noise. We want to emphasize the scale on this graphic view: we are talking about the second decimal point of the wavelength measured in nano-meters. Now, for example, we can see how this graph appears when the gluing is slowly collapsed:

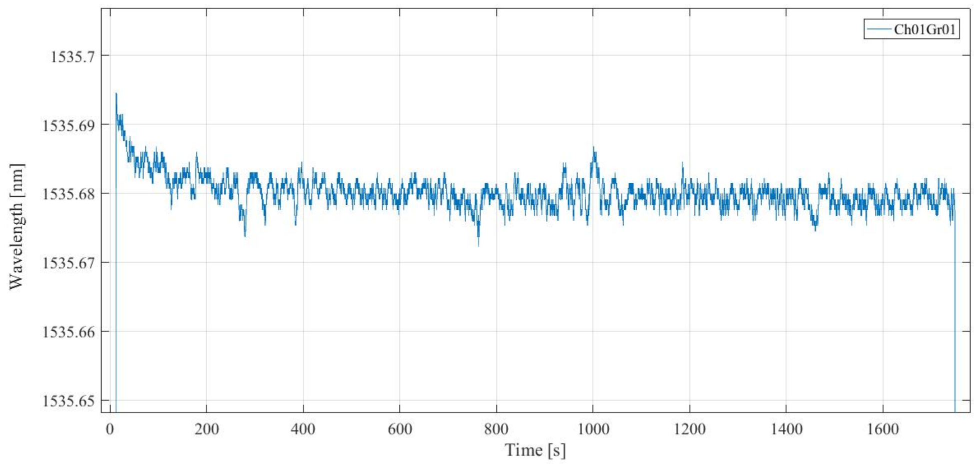

Figure 4.5: Example of a collapsing gluing

Even in this case we are talking about a very small accuracy, but it's important to notice that here the given position is reached in the first seconds but is not kept by the optical fiber after a long time. In other words we can see by this test that the wavelength read by the FBG is decreasing. It means that the optical fiber is slowly “sliding” on the plates, probably due to a not perfect gluing. Obviously this condition is not acceptable for our own tests.

Another type of test conducted has a similar goal: test and verify the goodness of the mechanical aspects of our system. In this case the idea is to understand the response of the system to frequent variations of the position in short periods of time. In particular, we decided to command a complete turn of the internal screw of the micro-translation (the same that in the previous case), alternating with the zero position every ten seconds. The path that we obtain is something like a “square wave” :

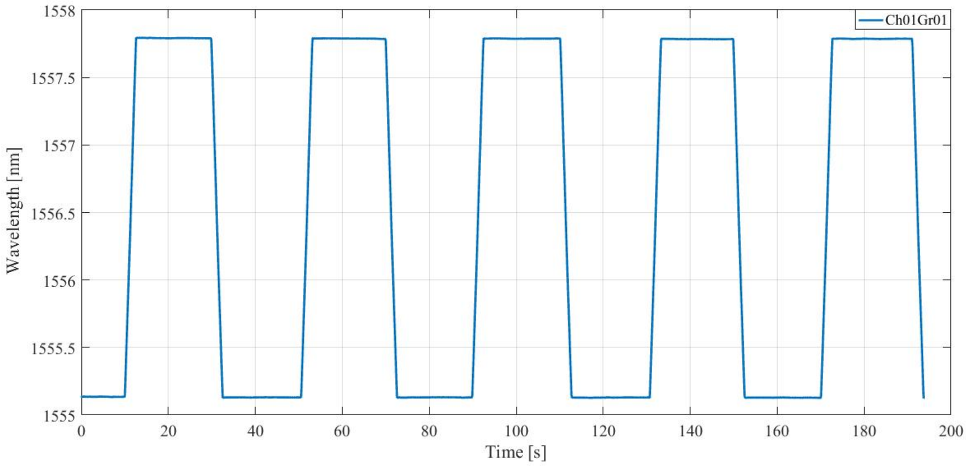

Figure 4.6: Square wave

Even in this case, we can zoom on the graph in order to see with major accuracy the response of the optical fiber. It’s good to see that every single time the final position reached is very similar to the previous one and that the wavelength does not change a lot into a single step (pay attention on the accuracy of the graph, again). Obviously, we can underline the same behaviour in the wavelength related to the zero position of the micro-translation:

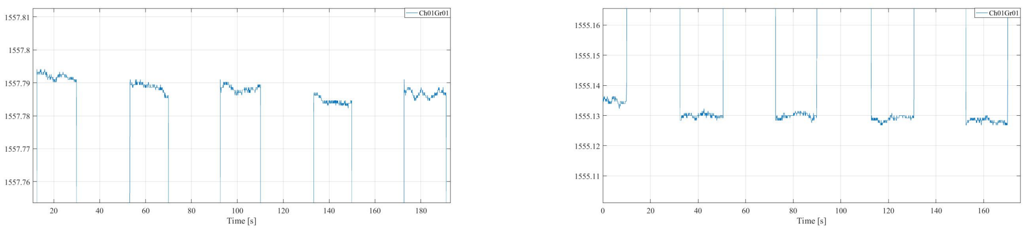

(a) *Top position*

(b) *Bottom position*

Figure 4.7: Zoom of the previous graph

Obviously both these behaviours are good for our own system, so we can start to execute tests, that are illustrated in the following paragraphs.

4.2 Measurements

So this tests campaign include a certain number of these tests, repeated in about a 3-months period. During this period the tests have been conducted almost daily and the most important quantities have been registered for every single test, numbering them with the current date, like in the example below:

Test	**Data collected**	[ ]
dd/mm/yy_#1	Start wavelength	*nm*
	Corrective factor, K	*adim*
	End wavelength	*nm*
	Temperature	$^\circ C$

Table 4.1: Data collected from the tests

It's important to specify that with the term *Start wavelength* we refer to the wavelength read (even by the interrogator) just before to start the specific test. Similarly we indicate with *End wavelength* the value given by the FBG when the micro-translation returned to zero position, so just at the end of the specific test. One of the most important parameter that has been considered is the *corrective factor, K*: in fact it represents the goodness of the response of all the system, from the gluing to the information given by the FBG. This term is calculated by the MATLAB script called *fitting.m* (described in the previous chapter) and it is based on a statistical analysis, as you can see in the graph below:

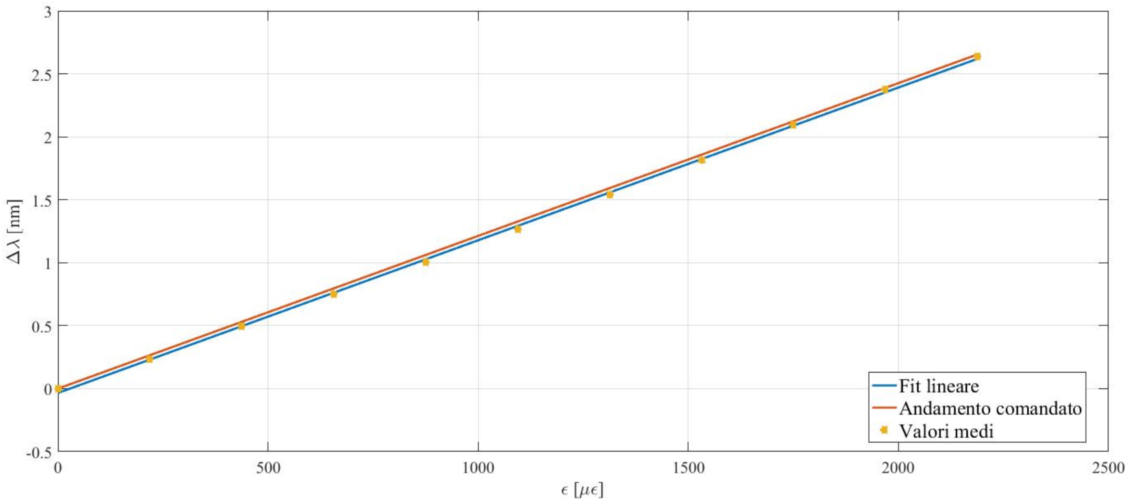

Figure 4.8: Example of statistical analysis to estimate K

It's easy to understand that, because of it is a corrective factor, it desirable for it to be as close as possible to the unit value. Generally, it is a quantification of all the viscous physical phenomena that affect our measurements, so we will see it easily with a set of graphs. For every single test that has been processed in fact, this value changes and, thanks to the MATLAB code *fitting.m*, we are able to see the differences before and after the application of the *corrective factor*.

1	Nome File	Pretensionamento [nm]	Fattore correttivo "k"	Post-tensionamento [nm]	
410		22/02/2019			Temperatura [° C]
411	22-02-19_1	1555,053	1,0659	1555,055	22,1
412	22-02-19_2	1555,055	1,0686	1555,056	22,3
413	22-02-19_3	1555,056	1,0679	1555,055	22,3
414	22-02-19_4	1555,055	1,0679	1555,055	22,3
415	22-02-19_5	1555,055	1,0694	1555,056	22,4
416	22-02-19_6	1555,056	1,0697	1555,055	22,6
417	22-02-19_7	1555,055	1,0708	1555,057	22,6
418	22-02-19_8	1555,053	1,0709	1555,055	22,6
419	22-02-19_9	1555,055	1,0738	1555,056	22,6
420	22-02-19_10	1555,056	1,0732	1555,055	22,6
421	22-02-19_11	1555,055	1,0723	1555,058	22,7
422	22-02-19_12	1555,056	1,0737	1555,058	22,7
423	22-02-19_13	1555,058	1,0739	1555,058	22,7
424	22-02-19_14	1555,058	1,0738	1555,058	22,9
425	22-02-19_15	1555,058	1,0731	1555,058	22,9
426	22-02-19_16	1555,058	1,0743	1555,057	22,9
427	22-02-19_17	1555,057	1,0749	1555,058	22,9
428	22-02-19_18	1555,058	1,0769	1555,058	22,9

Figure 4.9: Part of the excel file used to collect data

Obviously it's not possible to display here all the values obtained during all this analysis phase, with over 400 *tests* executed. An excel file exists to curry out this function, as shown in the previous picture. We will see in the following paragraph how all these data have been processed in order to bring out relevant information and observations.

4.3 Data Analysis

In this paragraph, the results obtained during the test campaign are described and commented. Firstly, we want to underline the type of the optical fiber used, in order to emphasize some particular characteristics:

Element	**Characteristic**
Type of the FBG	Periodic variation
Fiber's material	Polyimide
Effective Length	$L_0 = 228.94\ mm$
Center wavelength	$\lambda_0 = 1555.06\ nm$

Table 4.2: Specific characteristics of the optical fiber used to perform tests

So, using this optical fiber, with the support of all the hardware needed, we executed about 400 *tests* with the path described at the beginning of this chapter (cf. 4.1) and with the support of all the software mentioned above, we processed all data collected. At the end, a simple MATLAB script was created in order to plot all these information into some graphs. Focused on them, we will underline the relevant conclusions that it's possible to find out and we will comment particular behaviours of the optical fiber noticed during these tests.

First of all, considering an increasing chronological numeration of the tests, it's interesting to see how the corrective factor "K", described deeply in the previous paragraph, changes during the tests:

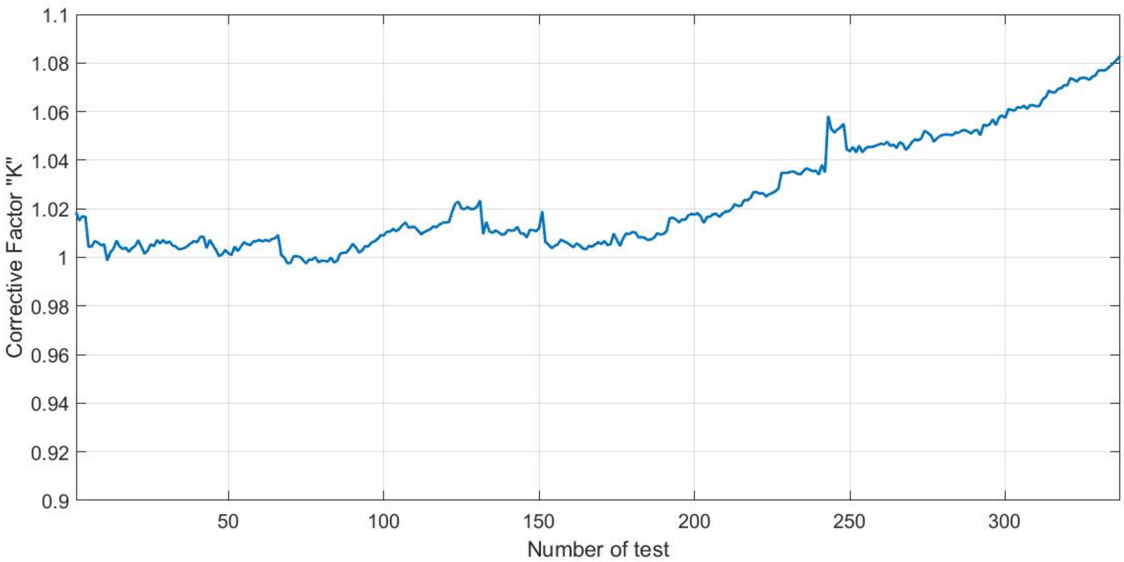

Figure 4.10: Total trend of the corrective factor "K"

Every single test, in fact, gave us a value of this corrective factor and it is near to the unit value when the measured data are very close to the theoretical ones, as shown in the picture below:

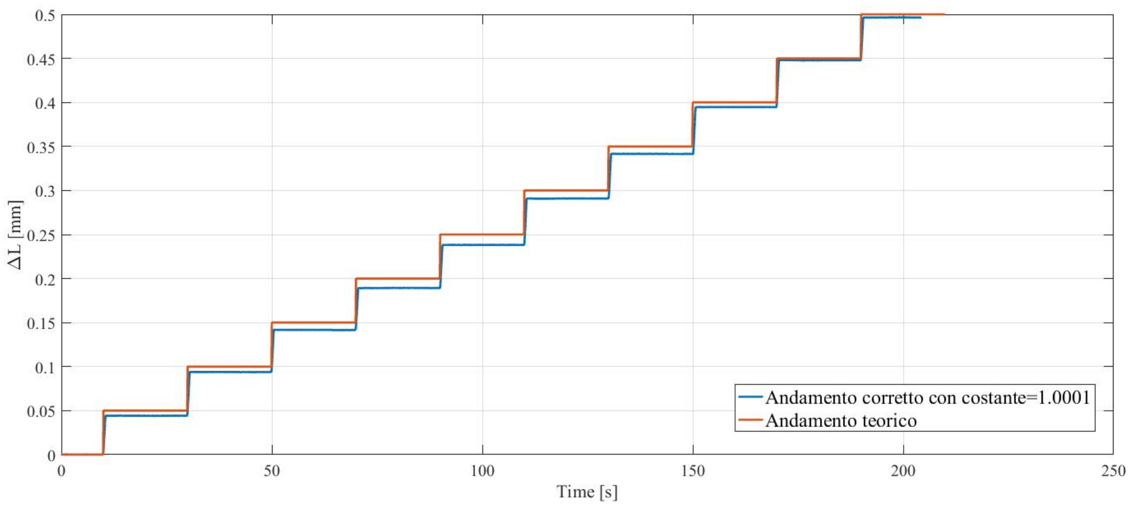

Figure 4.11: Example of a corrective factor $K = 1.0001$

The blue line represents the steps executed by our optical fiber and registered by the FBG sensor, the red one instead contains the theoretical and desired values. As you can image, this matching will be not present in all the other cases. The value of the corrective factor, in fact, depends on a lot of elements, that we will try to identify during our own analysis, always considering that other factors (such as external noises or a combination of viscous phenomena) are difficult to characterize or quantify. As mentioned above, it desirable for it to be as close as possible to the unit value and we will see that this condition is kept just in the first about 200 *tests* than it starts to diverge to elevate values (cf. 4.10).

So, starting from the graph above, we can underline some particular behaviours of our sensor. Firstly, we want emphasize in this case too (how we have done about the graphs of the wavelength seen before) the accuracy used to plot these values. Even if the oscillations of the "K" term seem important, the graph is limited (on the y axis) from the value 0.9 to the 1.1, so it's easy to understand that the variations between one value and the following one are about the third decimal point. Another important thing that it's possible to explain looking at this graph is about the value of the "K" factor at the end of one day tests and its value at the beginning of the following one. To underline what is happening, we decided to see in details the tests run in the first 6 *days*, in order to try to explain phenomena involved. So, in the picture below, we plotted only the first about 150 *tests* and we signed (using the dotted red lines) the transition between one day and the following one:

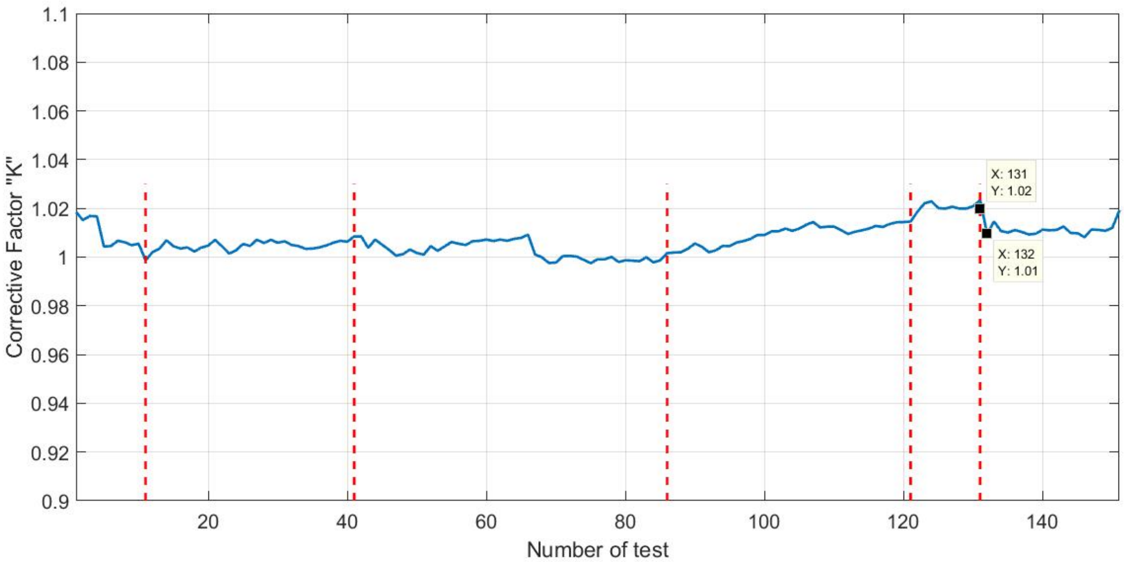

Figure 4.12: Trend of the corrective factor "K" in the first 6 *days*

It's possible to observe a particular phenomenon: in some days, the "K" term keeps its trend and it does not change a lot from one day to another. But in some particular cases it changes significantly, such as in the case underlined in the picture by the *MATLAB datatips*. In this situation the corrective factor went from 1.0234 to 1.0096 registered in the following test, before it starts to grow up again. It's easy to understand that in the accuracy that characterizes our field tests, this variation is not negligible. So, to try to understand what is happening to the optical fiber, could be useful to see the trend of the called *start wavelength* during this part of the tests. As explained above, we referred to *start wavelength* as the wavelength read by the *Dynamic FBG interrogator* just the moment before that specific test was run. Doing this, it's possible to see the similar trend that characterize wavelengths respect to the corrective factor. We can say that they "go together", i.e. if the start wavelength decreases also the corrective factor does it. In the same way, if the start wavelength is increasing, also the "K" grows up. Applying this reasoning to our graphs, we can see that when the corrective factor has an important change from one test to the following one, also in the trend of the wavelength we can underline the same behaviour:

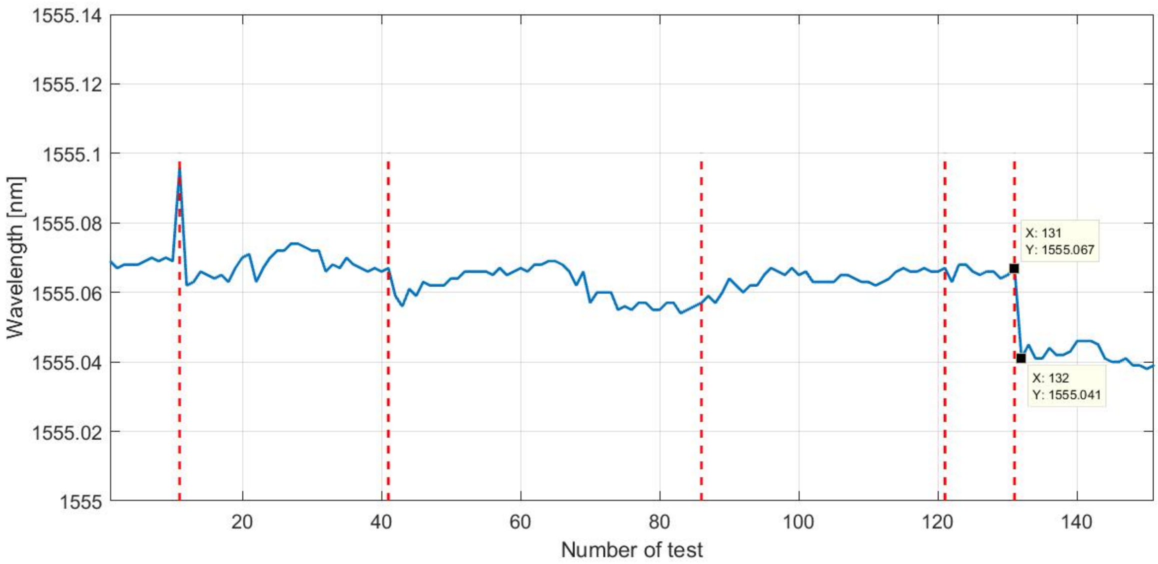

Figure 4.13: Trend of the wavelength in the first 6 *days*

Even in this case we emphasized the transition with dotted red lines and also in this graph (such as in the "K" trend) in the transition between the test number 131 and the 132 an important variation is registered. Here the start wavelength went from 1555.067 *nm* to 1555.041 *nm*, while in the other cases the trend was almost always constant (remembering the accuracy of the graph shown - we are talking about the second decimal point of a quantity measured in nano-meters).

4.3.1 Effects of the temperature

At this point of our important analysis, we tried to consider the phenomena involved that can cause these variations, taking always into account the viscous phenomena and the other random effects that we are not able to quantify. On the other hand, a physical quantity that we can measure and that certainly affected our tests is the temperature. For this reason, during all our measurements, a thermometer with an accuracy on the first decimal point has been used to monitoring the temperature into the enclosure in which the optical fiber has been mounted. Even in this case, we can use some graphs to explain how the temperature is related with the other quantities. At first, we thought that a relation between the corrective factor and the temperature could exists, so we tried to see it using the graph below:

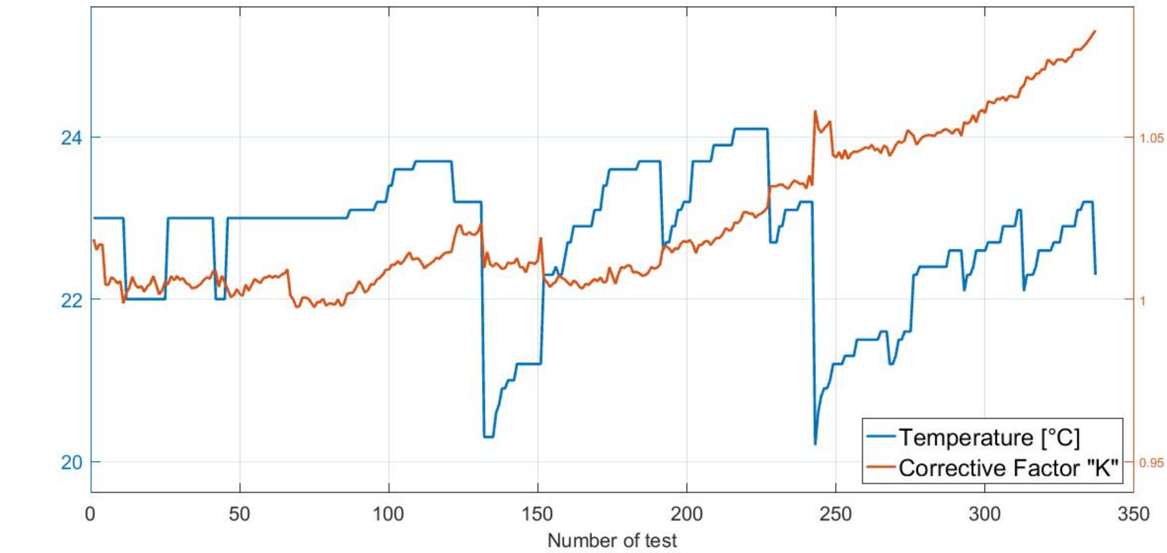

Figure 4.14: Trend of the temperature in relation with the corrective factor

At first sight, it might seem that a correlation between these two quantity does not exist. Really, it is intrinsic and it depends on the relation between the corrective factor "K" and the start wavelength measured. In order to explain this relation another graph as been plotted:

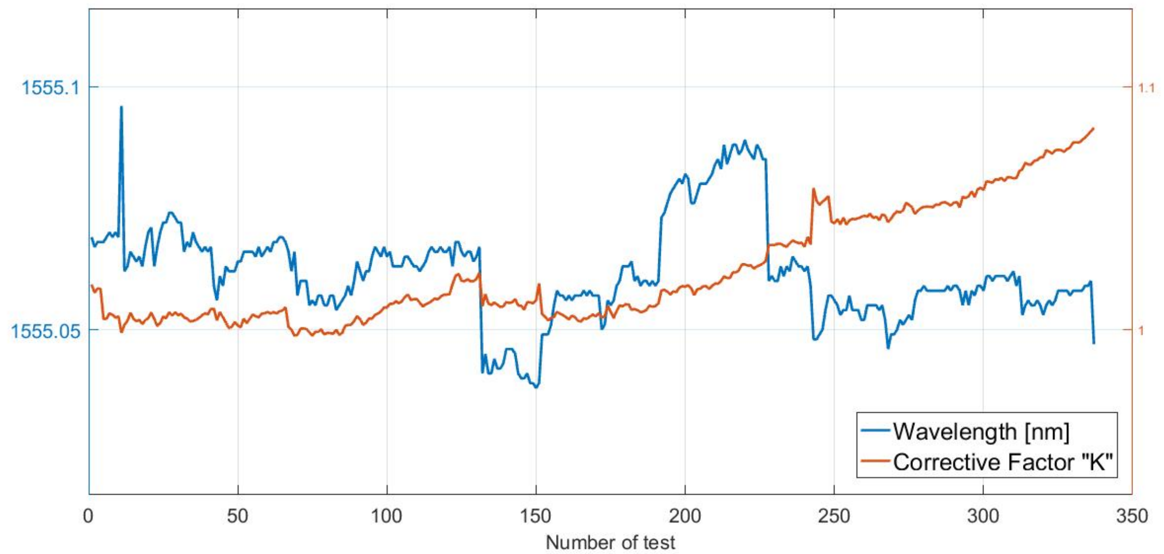

Figure 4.15: Trend of the corrective factor in relation with the start wavelength

It's clear from this picture that the corrective factor "K" is able to follow the trend of the wavelength to a certain point, fixed about the $200th\ test$. When the start wavelength decreases under a particular value, the corrective factor starts to diverge, moving away from the unit value. This behaviour is registered in particular way when the start wavelength is increasingly lower then its own center wavelength λ_0: the possible motivation of this behaviour will be explained soon.

So, remaining into the temperature problem, one of the most important relation found during these tests is clearly visible thanks to the following graph:

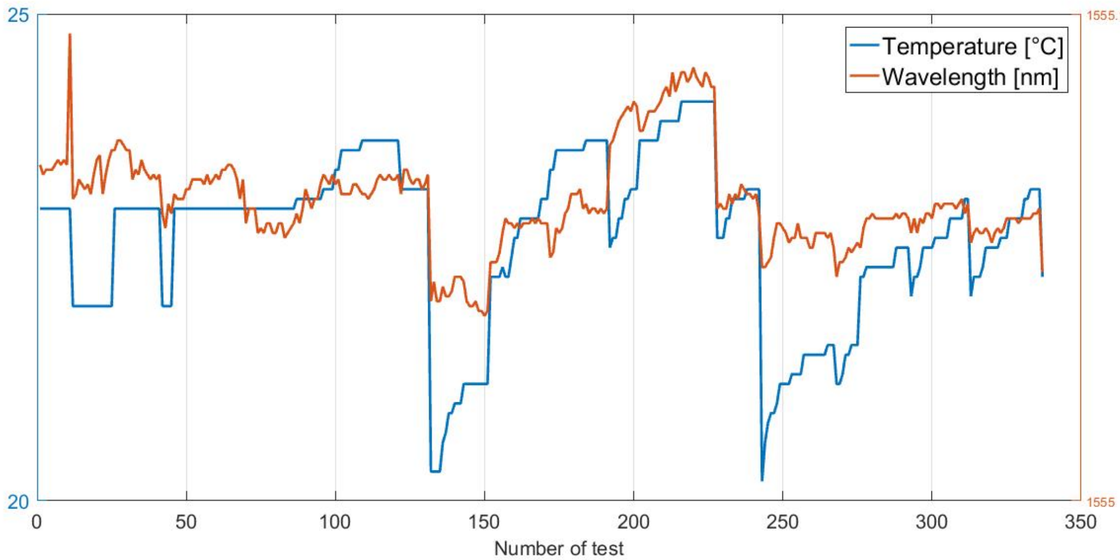

Figure 4.16: Trend of the temperature in relation with the start wavelength

From this picture, it's easy to observe that every single change in the temperature modifies the value of the wavelength read by the Bragg of the optical fiber, from the first test to the last one. This changes in turn affect the value of the corrective factor "K", as shown in the picture 4.15. At this point it's possible to explain why every change in temperature influences so strongly the value of the start wavelength. Taking always into account that there are some viscous phenomena that can not be controlled, such as the gradual collapsing of the Araldite and/or of the PLA plates, an important and quantifiable phenomenon occurs: the deformation of the Aluminium of the breadboard (base of the enclosure in which all the system has been fixed). This deformation, assumed linear in the mounting direction of the optical fiber, depends on three terms:

$$\Delta L = \alpha L_0 \Delta T$$

in which α is the *coefficient of linear thermal expansion* and for the Aluminium is $\alpha = 2.4\ 10^{-5}$. The variation of the temperature, considering in this case too the tests number 131 and 132, is in module $\Delta T = 3^\circ\ C$ and considering the total length between the points in which the fiber is fixed on the breadboard $L_0 = 275\ mm$, we obtain in module:

$$\Delta L = 0.0198\ mm$$

This calculation justifies the important variations registered in the wavelength when the temperature changes: the value obtained is a very little distance, but if we compare it with the precision of the system with which these tests have been performed, it assumes another importance. Just to give a reference value, we have to think about the path of the executed tests: a single step executed by the micro-translation has an amplitude of 0.05 mm and it causes a variation of the wavelength about 0.25 $nano-meters$ (cf. 4.2 e 4.1). So, a decreasing of about 3° C is fully consistent with a decreasing of the wavelength that goes from 1555.067 nm to 1555.041 nm:

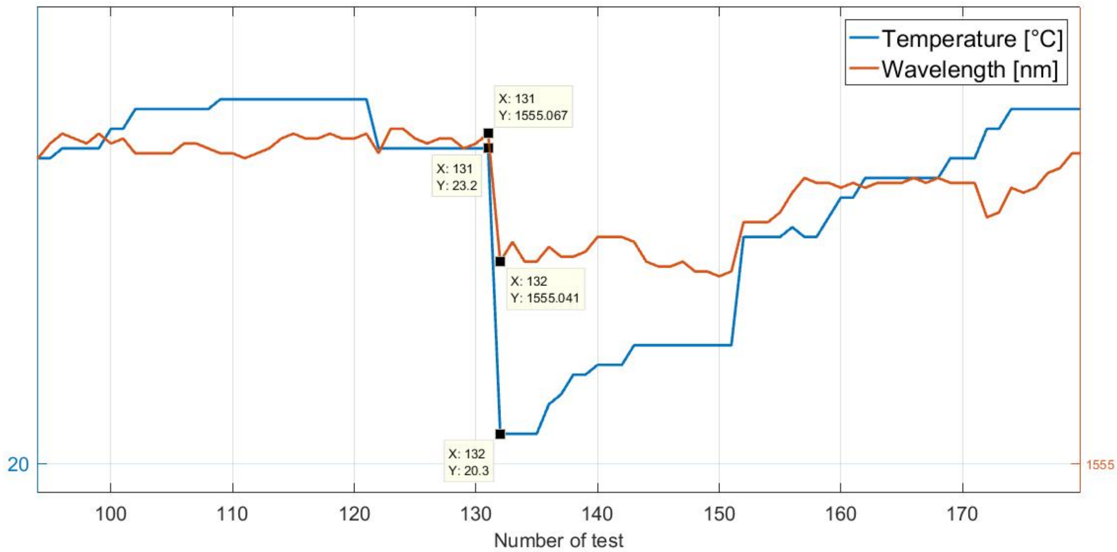

Figure 4.17: Relation between temperature and wavelength

Obviously as mentioned before, the variation of the wavelength (and in turn the variation of the corrective factor) does not correspond perfectly with the temperature variation, because of the other unquantifiable phenomena involved. At the end, in order to confirm these results, a particular graph has been created: all the start wavelengths measured have been plotted with the temperature and even if an important dispersion is visible, it's possible to find a generic trend:

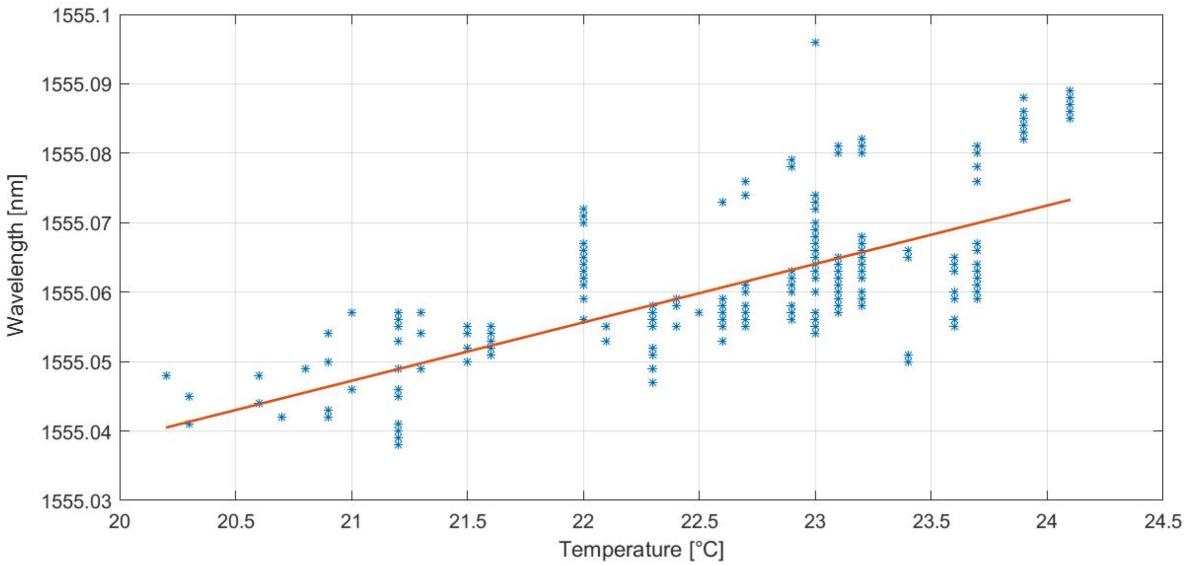

Figure 4.18: Dispersion of the wavelengths with temperature

4.3.2 Other effects

In this paragraph, other possible elements that affected all tests are detected. In some tests, for example another particular behaviour has been registered: if a major time passed, between one test and the following one, a variation in the wavelength read occurred, even if the temperature did not change: for example between the test number 276 and 277 one hour passed and the wavelength increased from 1555.052 nm to 1555.056 nm, even if the temperature was constant. In cases like this, probably the cause is to impute to all phenomena that we are not able to measure, such as the humidity effect in the glue or the mechanical collapsing of the system in general.

Another fundamental observation can be done about the graph 4.15: as briefly said before, the start wavelength reaches a value too low, if compared with the center wavelength of the optical fiber $\lambda_0 = 1555.06$ nm. For example, when the corrective factor "K" started to diverge, moving away from the unit value, the first step of our path used to perform tests, became smaller test after test. We can notice from the graphs below (in which the corrective factor was about the value 1.0219) how they change because of the system is starting to collapse:

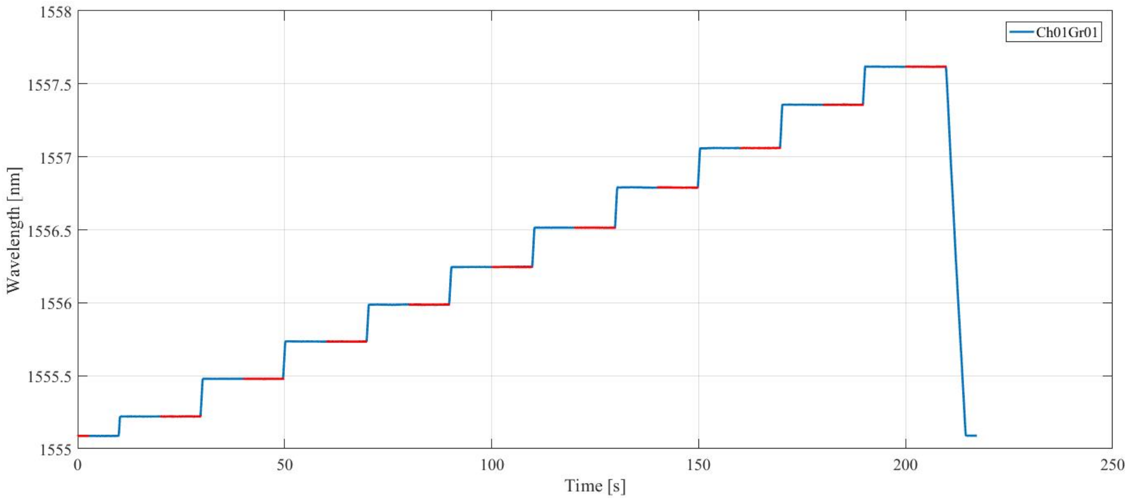

Figure 4.19: Trend of the wavelength during time

The other graphs used to analyse data are the following:

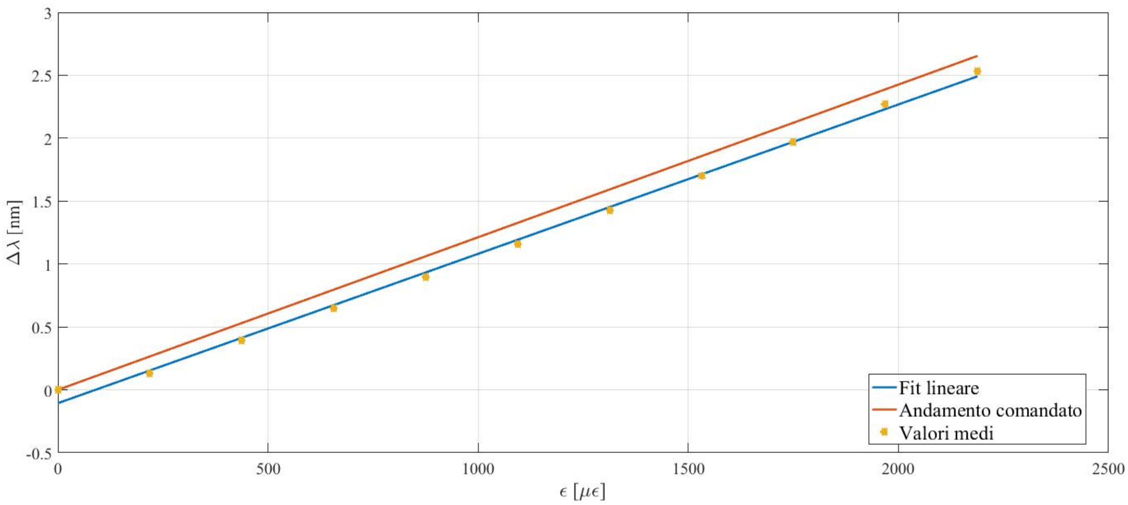

Figure 4.20: Fit to estimate corrective factor

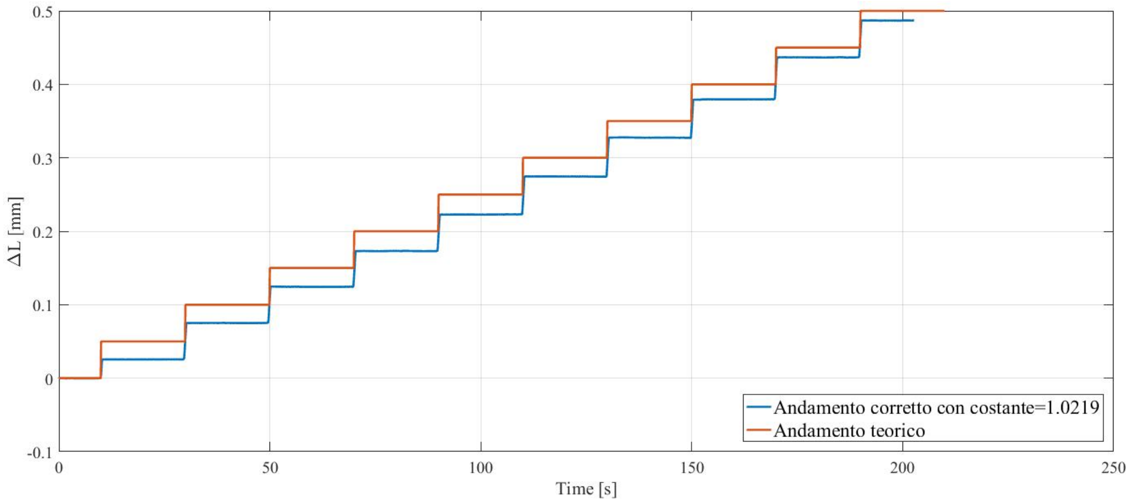

Figure 4.21: Comparison between theoretical and real data

This phenomenon is ever more visible continuing to stress the optical fiber and increasing the number of tests executed. So, if we do not intervene increasing manually the tension in order to grow up the start wavelength, the value of the corrective factor "K" is not able to keep itself about the unit value. This situation obviously affe5cts the trend of the tests and it degenerates after a certain number of tests, as we can observe in the graph below:

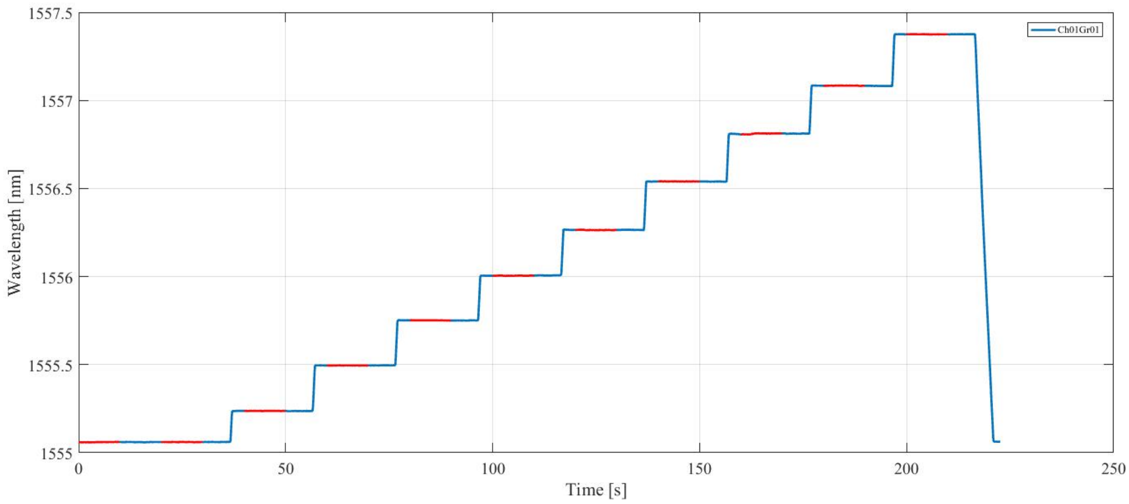

Figure 4.22: Trend of one of the last tests

This picture shows what happened in one of the last tests performed: because of the start wavelength was too low, the first step done by the micro-translation is not sufficient to reach the desired value. In fact, it's easy to notice by the picture above that the first step practically no longer exists. At this point, this behaviour is perfectly understandable: the first step commanded "is used" by the optical fiber to reach its own center wavelength so we can say that the FBG sensor is not working in the right way. In other words, the stress given to it with the first step is necessary to return to a correct stretch, so that part of the stress imposed by the micro-translation is not read by the sensor. This explanation is the reason why doing more and more tests the value of the corrective factor is even more high: the optical fiber is slowly sliding on the plates (so the start wavelength became too low) and it is losing its tension given to it in the gluing process. A demonstration of this phenomenon is visible when we compared the trend seen above with the desired values, in order to estimate the corrective factor:

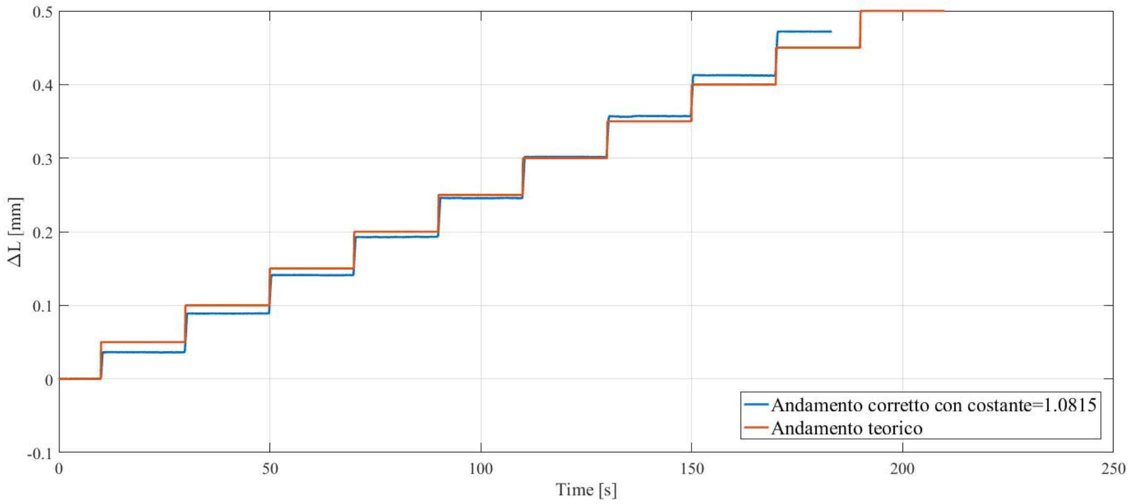

Figure 4.23: Comparison between the desirables and obtained values - with the modified MATLAB script

Practically, the value of the corrective factor is too high because the first theoretical step is compared with the second step of the practical measurements. In fact, you can notice that the steps in blue are just nine in the graph above, because of the first part (visible in the figure 4.22) has been cut graphically from the MATLAB script, because of its constant trend. This happened because of the changes described in the paragraph 3.3.2 about the need to obtain a perfect matching between the first steps theoretical and effectively measured. We want to remember that this change affects only the graph, all the values calculated by the script (including the corrective factor) do not change. If you plot this behaviour with not introduce this change to the MATLAB script, what you obtain is the graph below:

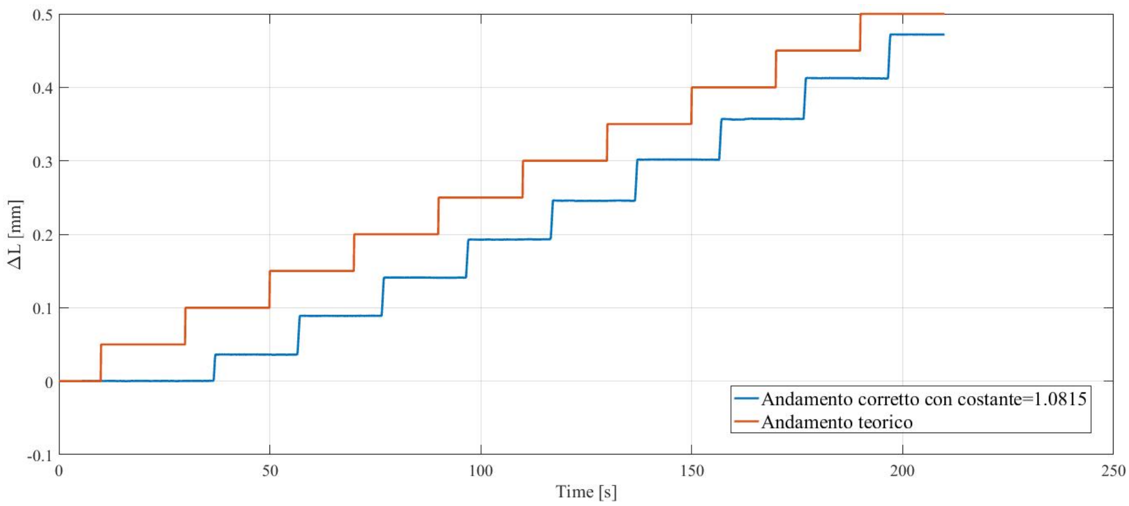

Figure 4.24: Comparison between the desirables and obtained values

So, we can conclude this repeatability test campaign saying that to a certain point, the information read by the FBG sensor are precise and accurate, but after a certain number of stresses imposed on the system, it needs a manual intervention in order to re-stabilise the initial parameters.

Obviously, this considerations have been done with our own external conditions, with a particular value of strain imposed for every single test and with the particular path described. Modifying even one of these elements the results could change: for this reason, we refers the reader to the Appendix for other observations done about it.

Chapter 5

Conclusions and Future work

In this chapter, we will summarise the results obtained with this test campaign, so we will underline the goals that have been reached and the new information obtained about the behaviour of the optical fibers used as sensors. Morever, it's important to remember that all these tests have been conducted considering a future possibility to really install the optical fibers on a aeronautic vehicle, using them in place of the actual sensors.

5.1 Conclusions

At the end of this thesis work, it is possible to summarise a lot of important information assimilated during these tests. The optical fibers represent innovative and very reliable elements for the future of the aerospace. All their advantages have been deeply described in the previous chapters and, even if they have some disadvantages, during this test campaign their importance and reliability have been totally demonstrated.
First of all, the work related to assembly the test bench, for example the process to fix the fiber on the plates using Araldite, has been a formative and fundamental part of this work. Moreover, the tests performed gave us very confident results and they showed the excellent performances of the FBG sensors. The optical fibers demonstrated they are able to not change their behaviour for a large number of repetitive tests. Even in that cases in which the values of the quantities analysed were not perfectly correspondent with the predicted values, in fact, they however showed some important phenomenon to detect. The most important result we obtained, as deeply explained during this thesis, is the relation between two important quantities involved: the wavelength at rest with the variation of the temperature. Indeed, other viscous phenomena that could not be controlled and measured during this work could be taken into account in the future. Certainly much work remains to be done, in order to make the entire system more stable and reliable.

At the end, we want to emphasize the accuracy of all the system. So, the results obtained compared with the precision used to execute all measurements and analyses, assume another relevance.

5.2 Future developments

In order to better understand how much all the viscous phenomena influence the sensors, should be useful to execute other tests campaign, applying some changes:

- *To monitor moisture changes:* all these tests have been performed monitoring the temperature changes into the plexiglass enclosure. It should be useful to monitoring the moisture content of the air too, in order to understand if it can influence response of the FBG. It might prejudice even the quality of the glue, so it can cause (with the others) some viscous phenomenon.
- *To change system temperature:* it's possible to repeat these tests imposing a different temperature from the ambient temperature. An idea could be to heat or to cool the total system and, considering even the deformation caused on the breadboard, analyse the behaviour of the Bragg. Should be better to monitor and control the moisture content of the air too. In this case, it could be necessary to validate a relation between the variation of wavelength with the variation of temperature, first of all with static tests (see the work described in Appendix B).
- *To execute an higher total number of tests.* It could be interesting to see the behaviour of the optical fiber when stressed with ah higher number of repetitive tests. The idea could be to verify if it reaches a fatigue failure or not.
- *To apply less deformations:* we measured the deformation applied during these tests in the previous chapter in terms of *microstrain*. It's possible to repeat the tests imposing a minor deformation or, if you want, using a major total length of the fiber. In this way it's possible, even controlling and monitoring temperature (and moisture content too), to understand if the appearance of viscous phenomena (first of all, viscous creep) seen in these tests can be delayed.
- *To measure strain direclty by the interrogator.* How explained during all this work, we measured just the wavelength, using the FBG of the optical fiber, read by the *Dynamic interrogator* and then we analysed the obtained responses using other software (MATLAB in our own case). An idea should be to repeat these tests reading the strain directly by the interrogator, correctly setted. As already described in greater details, in fact it's possible to use the Bragg of the optical fiber as strain sensor, so you can find new information without the need to know the different wavelengths.
- *To change method of gluing.* Using the same epoxy resin, into our own laboratory new gluing methods have been created recently, that guarantee a better position of the fiber on the plates and a minor quantity of resin. These elements, added to the other seen before, should contribute to have better results and/or should show optimum behaviour both of the FBG and the total system.

Appendix A

Different Path

This part of this thesis work has been written in order to not burden the reader during the description of the tests campaign and the observations of the results obtained. However, a little number of another type of tests have been performed, so we want to explain their development and what we obtained from them.

Something about 25 *tests* have been conducted, at the end of the 400 *tests* described, in order to verify if a different path used to perform tests could change the results. So we decided to reverse the execution steps. In other words, using directly the ARDUINO software, we drove the micro-translation immediately to the final position, fixed during all tests campaign at 0.5 mm and starting from this position we commanded to going down through the same steps of 0.05 mm. As you can image, what we obtained are reversed graphics that, in terms of wavelength are like in the picture below:

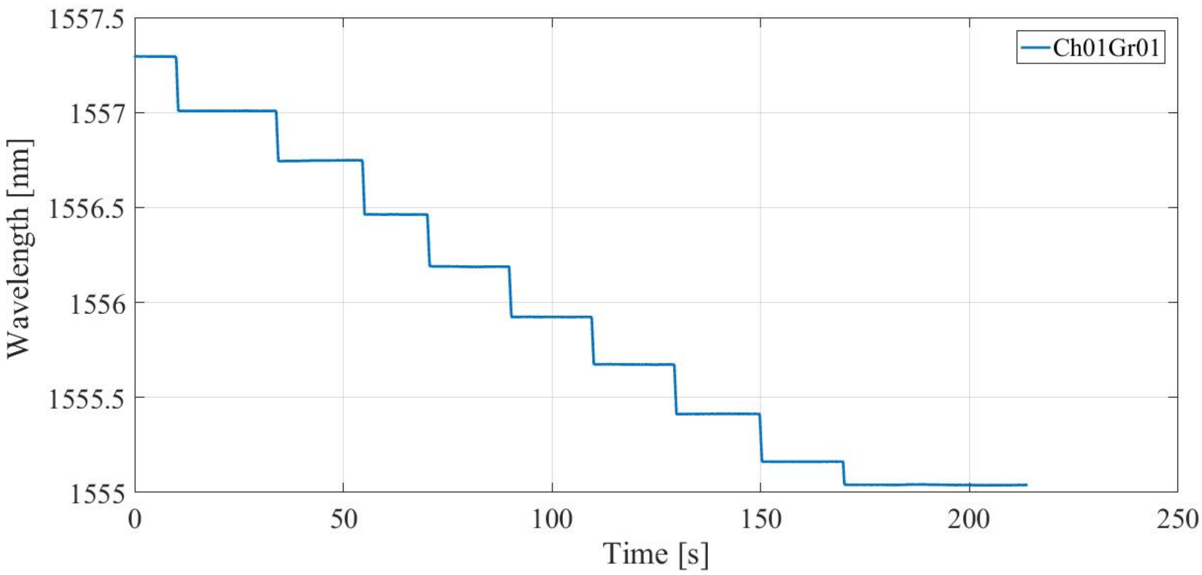

Figure A.1: Example of a “reversed” test

In this case too, the results have been collected into the same excel file used for all the other tests (cf. 4.9). So, even in this case we used MATLAB to plot all these data into some graphs, using which we have been able to do some observations.

First of all, we want to underline that the behaviour of the corrective factor does not change with these type of tests. In the following picture in fact we can see how it continues to diverge to high values, for all the reasons explained in the *chapter 4 ("Tests and results")*:

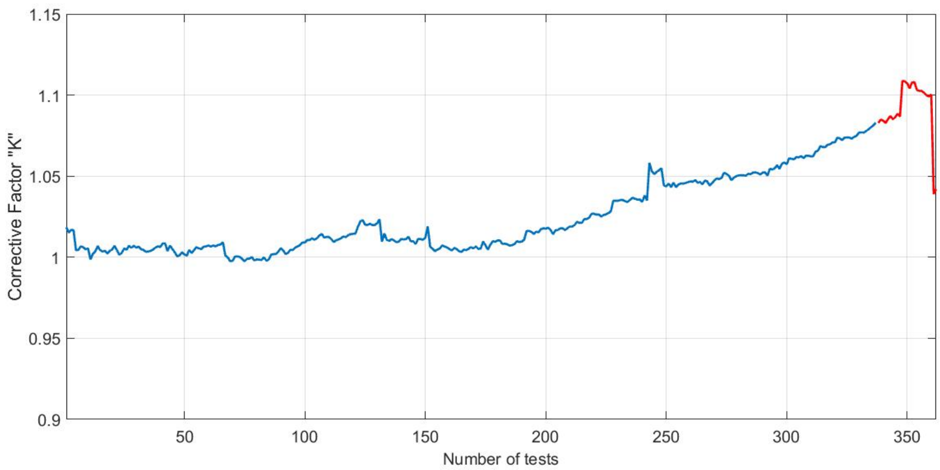

Figure A.2: Total trend of the corrective factor

In order to show better the importance of the values assumed by the corrective factor "K" in this part of the analysis, we decided to plot them as a natural follow-up of the previous tests performed, using the red line to individuate them easily. As it's possible to notice, in fact, even if the tests have been conducted in reverse, the behaviour of the optical fiber has not changed and the value of the corrective factor keeps to diverge.

As seen with tests performed during our campaign, when the value of the start wavelength, registered just before to activate the micro-translation, became too low, the first step of the analysis disappear and it caused the growing up of the corrective factor. In this case we can observe this phenomenon in the last step (instead that in the first one). This last step became so little that the FBG sensor is not able to sense a different wavelength, so as it is possible to see in the graph below, the total number of steps is nine and not ten, as we commanded to the micro-translation:

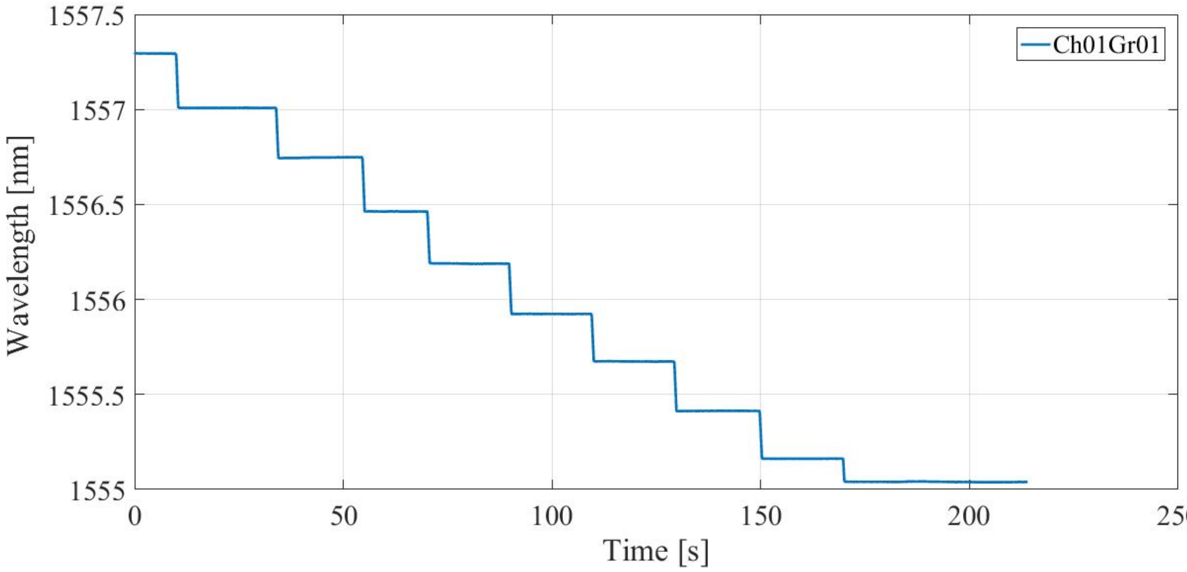

Figure A.3: Trend of wavelength with "reversed" test

This behaviour became even more clear when we calculated the corrective factor "K". In fact, it's possible to observe in the picture below the behaviour previous described: the last step is not even registered by the FBG sensor:

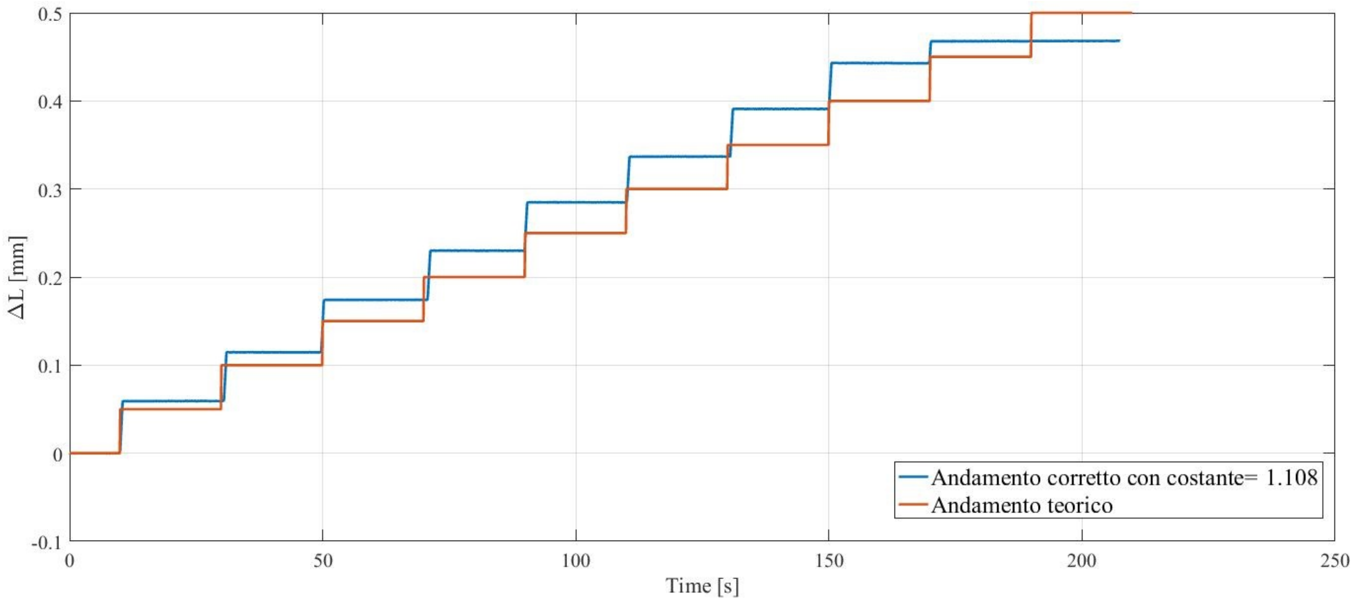

Figure A.4: Estimation of the corrective factor with "reversed" test

We want to underline that when the MATLAB script *fitting.m* processes data, it is able to rotate (graphically) the steps executed, in order to compare the values measured with theoretically values. So even if the steps are executed in reverse with respect with tests performed during this thesis work, in this graph they appear rotated.

At the end, we can do the same considerations done in the *chapter 4 ("Tests and results")* about the relation between the start wavelength of every single test and the temperature measured into the enclosure. Even with this type of tests the trend of these two quantities are very similar, so we can confirm how much temperature influences our tests:

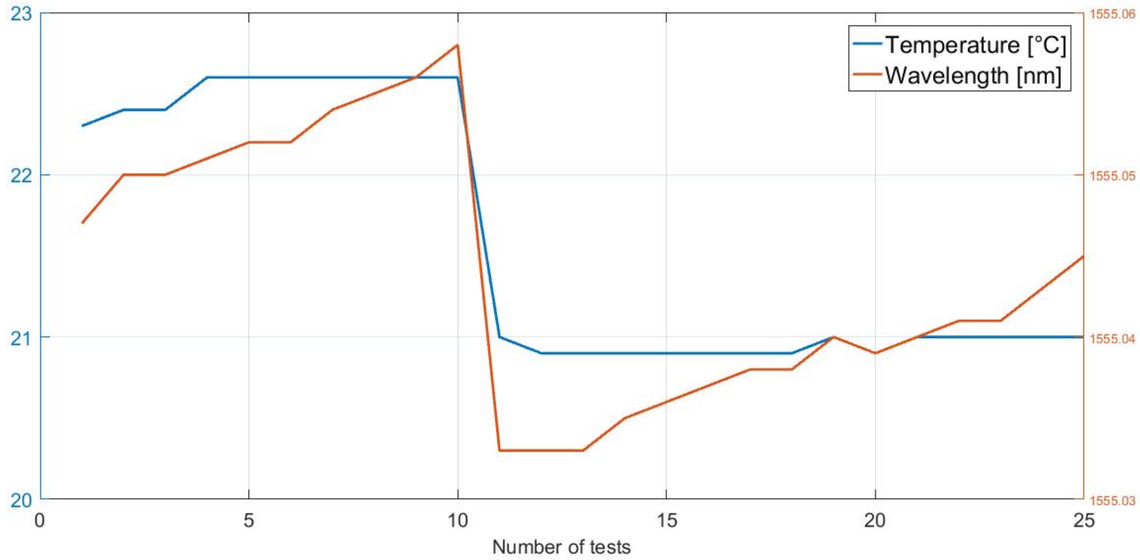

Figure A.5: Relation between temperature and start wavelength in the “reversed” tests

In this graph too in fact we showed how temperature changed and with it the wavelength does it too. About the test *number* 20 they have even a perfect matching.

Appendix B

Related Work by Team Icarus

In this part of this work, we want to describe and summarise a part of the tests performed by *Team Icarus* (a student team of our *Politecnico di Torino*) into the same enclosure used to perform all the other tests and with all the same equipments. These tests have been conducted a few weeks before our own tests and they are static tests. We want to refer to them, because we can do some observations that can confirm what we found from our data analysis. All the pictures and graphs used in this appendix, have been provided from the *Team Icarus*, whom we thank.

Focusing on this test campaign, *Team Icarus* used three different optical fibers, fixed on three different micro-translations and with three different types of glue. Particularly, two fibers with a coating in acrylate have been fixed in two different ways: one with a particular epoxy resin (property of the team) and the other one with cyanoacrylate. Obviously, considering the gluing process of our tests, we can not refer to these two optical fibers, because of the different type of glue and coating could change the results. So we will use just the results obtained by the tests performed on the last optical fiber: it has a coating in polyimide and it was fixed on the micro-translation with the araldite (the gluing process has been executed about a month before to start tests). At the end, we want to emphasize that these tests have been performed with manual micro-translation, instead that the electric one used for our own tests. The picture below shows the three manual micro-translations with the three different optical fibers:

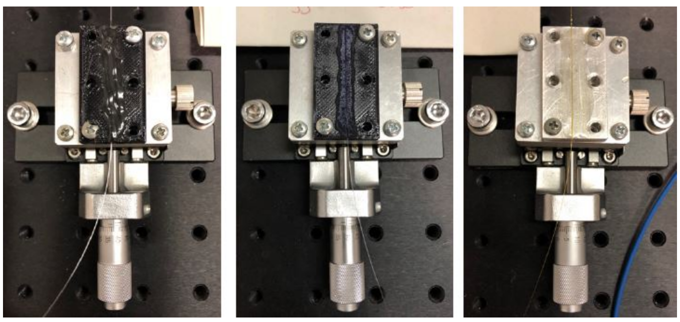

Figure B.1: Starting from the left: fiber in acrylate with epoxy resin; fiber in acrylate with cyanoacrylate; fiber in polyimide with araldite

It's possible to see from the picture above that the optical fiber of our interest is the third (starting from the left). This test campaign had a total duration of about

40 *days*: at the beginning the variations in terms of temperature and humidity was not monitored, so the first part of the tests (about the first 7 days) are not considered. Starting from this point, an analysis of the ambient conditions has been executed, in order to better understand the behaviour of the optical fiber, so both temperature and humidity changes have been registered:

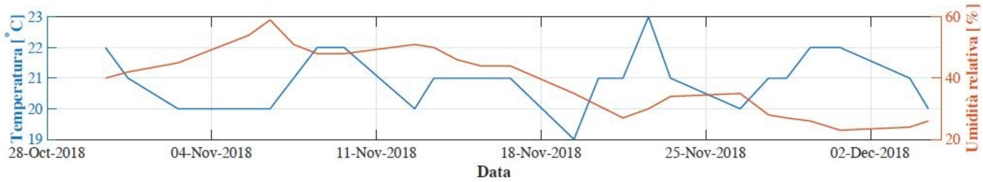

Figure B.2: Trend of the temperature and humidity

Starting from an equivalent length of $L_0 = 128.2\ mm$, the fiber of our interest (the in polyimide one) has been pre-loaded of about 5400 $\mu\epsilon$ (0.75 mm) and for the first about 20 *days* the position of the micro-translation has not been changed any more. After that, the micro-translation was moved to 0.55 mm, so the strain measured on the fiber was about 4150 $\mu\epsilon$.

For the convenience of the reader we can summarise all these information in the table below:

Element	**Characteristics**
Coating material	Polyimide
Type of glue	Epoxy Resin: Araldite
Effective length	$L_0 = 128.20\ mm$
Natural wavelength	$\lambda_0 = 1533.01\ nm$
First stretch	0.75 mm
	5400 $\mu\epsilon$
Second stretch	0.55 mm
	4150 $\mu\epsilon$

Table B.1: Summarise of characteristics of the test campaign executed by *Team Icarus*

For the reasons explained before, the graphs we will use to describe these tests have been split in two parts, in order to mark the different strain. First of all we can see a graph in which the value of the strain measured (compared to the initial one) have been plotted:

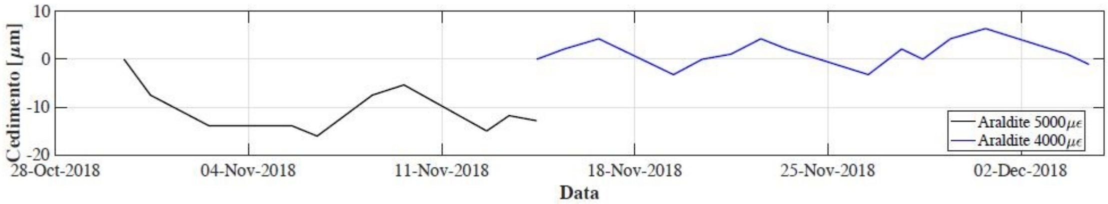

Figure B.3: Trend of strain during all the test campaign

As mentioned before, there are two curves (and not just one) in order to emphasize the different strain applied. We can see from this graph that, as explained and verified during our thesis work, even if the position of the micro-translation as not changed, the value read by the FBG sensor in terms of wavelength is not the same. This phenomenon depends to all the elements we described in the *chapter 4 ("Tests and Results")* and this is the reason why the tests conducted by the *Team Icarus* are so important. They are static tests and they demonstrated that a lot of phenomena affects the measurements and not always these phenomena can be controlled or monitored.

However, also in this case an important information is found comparing the trend of the temperature with the trend of the "λ failure". We indicated with this term the difference measured every day in the wavelength respect of the initial one (fixed at 1540.52 *nm* in the first part and at 1539.02 *nm* in the second part). These information are visible in the graphs below:

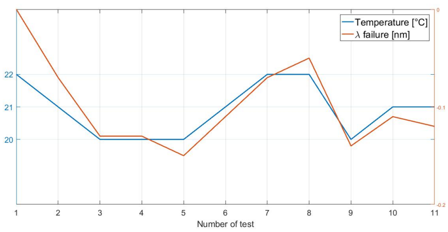

(a) First part of the test compaign

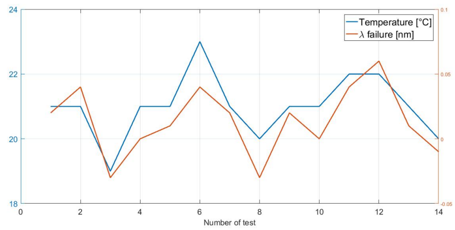

(b) Second part of the test compaign

Figure B.4: Trend of the temperature compared with wavelength

It's possible to see in these graphs, how important is the relations between these two quantities. So even in these case, we want to emphasize how important has been to compare this work executed by *Team Icarus* in order to confirm our own thesis work. At the end, we want to report here the values in wavelength terms registered by the FBG sensor in a few important moments of the test campaign:

Situation	Wavelength [nm]
Natural	1533.01 *nm*
First measure	1534.05 *nm*
First stretch	1540.52 *mm*
Second stretch	1539.02 *nm*
End of tests	1533.89 *mm*

Table B.2: Summarise of wavelengths measured during tests

As you can see in the table above, at the end of these about 40 *days* the micro-translations have been moved again to their initial position, so they were able to register the wavelength read by the FBG sensor.

At the end of this work, we can conclude that, as predict during our own work, temperature affects the measurement because the Aluminium of the breadboard deforms itself. Certainly, also the changing in humidity affects the system, probably intervening on the good behaviour of the glue. Moreover, a lot of unquantifiable and uncontrollable phenomena occur.

Bibliography

[1] G. Candiano, “Fiber Bragg Grating Sensors for Mechanical and Thermal Prognostics and Diagnostics for Aerospace Applications”, July 2018

[2] M. Yamane, Y. Asahara, “Glasses for photonics”, published by the Press Syndicate of the University of Cambridge, 2000.

[3] Wikipedia (2019), “Fiber Bragg grating”, $https://en.wikipedia.org/wiki/Fiber\_Bragg\_grating$